NUMERICAL ANALYSIS OF LASER DIODE ELECTRO-OPTICAL CHARACTERISTICS IN THE VICINITY OF LASING THRESHOLD

By

OKUNADE, IBRAHIM OLUSOLA

A THESIS SUBMITTED TO THE POST-GRADUATE SCHOOL, AHMADU BELLO UNIVERSITY, ZARIA IN PARTIAL FULFILMENT OF THE REQUIREMENTS FOR THE DEGREE OF MASTER OF SCIENCE IN PHYSICS.

DEPARTMENT OF PHYSICS
FACULTY OF SCIENCE
AHMADU BELLO UNIVERSITY
ZARIA - NIGERIA.

DECLARATION

I hereby declare that the contents of this work are the original work of the author and has not been accepted in any previous application for higher degree. All the sources of information are properly referenced.

This thesis entitled "Numerical Analysis of Laser Diode Electro-optical Characteristics in the Vicinity of Lasing Threshold" by Okunade, Ibrahim Olusola meets the regulations governing the award of the degree of M.Sc. Physics of Ahmadu Bello University and is approved for its contribution to knowledge and literary presentation.

Chairman, Supervisory Committee — Date 18/9/89

Member, Supervisory Committee — Date 10/10/89

Head of Department — Date 10/10/89

Dean, Postgraduate School — Date 12-1-90

ACKNOWLEDGEMENTS

Firstly, I am most grateful to God Almighty for sparing my life and making the completion of this work a reality.

My profound gratitude also goes to my supervisor, Dr. Z.O. Oyedokun for initiating this research and for his guidance and assistance throughout the duration of this work. I am also indebted to my co-supervisor, Dr. J.O. Adetunji, for his suggestions and critical review of this work.

Further, my appreciation goes to the Centre for Energy Research and Training (C.E.R.T.) for the use of some of their facilities.

Finally, my special thanks go to all members of my family, friends and working colleagues for their concern, love and encouragement during the difficult times in the course of this work.

ABSTRACT

The behaviour of laser diode in the vicinity of the lasing threshold was investigated using numerical methods. Polynomial equations were fitted to the electro-optical characteristics of the laser and the temperature variation of the coefficients of these fits were related to temperature dependent parameters of the laser. The approximate values of the threshold current was also determined from these coefficients.

A novel method of presenting laser characteristics called Temperature-current characteristics was further derived from Light-current characteristics by linear interpolation and approximate values of the temperature sensitivity of the laser was determined from this characteristics.

TABLE OF CONTENTS

		Page
Title Page		(i)
Declaration		(ii)
Certification		(iii)
Acknowledgements		(iv)
Abstract		(v)
Table of Contents		(vi)
1	INTRODUCTION	1
2	PRINCIPLE OF OPERATION OF SEMICONDUCTOR LASER DIODES AND THEIR ELECTRO-OPTICAL CHARACTERISTICS	6
2.1	General Considerations	6
2.2	Heterostructure confinement	7
2.3	Lateral confinement	9
2.4	Feedback and Frequency Selection	10
2.5	Semiconductor Materials for Lasers	12
2.6	Electro-optical Characteristics of Laser Diodes	13
3.0	NUMERICAL ANALYSIS OF LASER DIODE ELECTRO-OPTICAL CHARACTERISTICS	20
3.1	Numerical Analysis of Experimental Data	20
3.2	Polynomial Representation of Electro-optical Characteristics of the Laser Diode	21
3.2.1	Application of Polynomial Curve-fitting to Laser Electro-optical Characteristics	24
3.3	Deduction of Temperature-Current Characteristics from Light-Current Characteristics by Linear Interpolation	37

		page
4	RESULTS AND DISCUSSION	45
4.1	Determination of Threshold Current from Coefficients of the Fitting Polynomial.....	45
4.2	Variation of Coefficients A_i of the Fitting Polynomial with Temperature.....	45
4.2.1	Variation of Polynomial Coefficients with Temperature for L-I Characteristics.....	45
4.2.2	Variation of Polynomial Coefficients with Temperature for L-V Characteristics.....	54
4.2.3	Variation of Polynomial Coefficients with Temperature for I-V Characteristics.....	54
4.3	Predictability of Temperature Sensitivity of Laser Diode from Temperature-Current Characteristics	55
4.4	DISCUSSION	57
5	CONCLUSION	58

LIST OF TABLES

Page

Table 3.1: Variation of the coefficients of the fitting polynomial with temperature for L-I Characteristics for (a) GaAlAs (STC) laser (b) GaAlAs (LS) laser (c) GaInAsP (S_2) laser and (d) GaInAsP (LW) laser. 26

Table 3.2: Variation of the coefficients of the fitting polynomial with temperature for L-V Characteristics for (a) GaAlAs (STC) laser (b) GaAlAs (LS) laser (c) GaInAsP (S_2) laser and (d) GaInAsP (LW) laser. 28

Table 3.3: Variation of the coefficients of the fitting polynomial with temperature for I-V Characteristics for (a) GaAlAs (STC) laser (b) GaAlAs (LS) laser (c) GaInAsP (S_2) laser and (d) GaInAsP (LW) laser. 30

Table 3.4: Comparison of experimental L-I Characteristics data with calculated values for a GaAlAs laser at 10.2°C. The calculated values of d^2L/dI^2 are also shown. 33

Table 3.5: Comparison of experimental L-I Characteristics data with calculated values for a GaInAsP laser at 10.1°C. The calculated value of d^2L/dI^2 are also shown. 34

Table 3.6: Temperature-current characteristics data for GaAlAs ternary lasers. 39

Page

Table 3.7: Temperature-current characteristics data for GaInAsP quarternary lasers. 41

Table 4.1: Comparison of calculated value of threshold current from equation (4-6) with experimental values at various temperatures for (a) GaInAsP and (b) GaAlAs lasers. 47

LIST OF FIGURES

page

Figure 1.1: (a) InP/GaInAsP 20 μm oxide Stripe laser (b) Automatic CW L-I-V-T measurement of a laser. 2

Figure 2.1: Light output vs current characteristics for (a) GaAlAs and (b) GaInAsP lasers. 15

Figure 2.2: Light output vs voltage characteristics for (a) GaAlAs and (b) GaInAsP lasers. 16

Figure 2.3: Current vs Voltage characteristics for (a) GaAlAs (STC) and (b) GaInAsP (S_2) lasers. 17

Figure 3.1: Comparison of experimental and theoretical values for L-I Characteristics for (a) GaInAsP and (b) GaAlAs lasers. 35

Figure 3.2: Variation of d^2L/dI^2 with the drive current for (a) GaInAsP and (b) GaAlAs lasers. 36

Figure 3.3: Variation of temperature with drive current for various values of light output for (a) GaAlAs Ternary laser and (b) GaInAsP quarternary laser. 44

Figure 4.1: Variation of polynomial coefficients (a) A_o (b) A_1 (c) A_2 with temperature for L-I Characteristics for 2 ternary (LS, STC) and 2 quarternary (S_2, LW) lasers. 49

Figure 4.2: Variation of polynomial coefficients (a) A_3 (b) A_4 with temperature for L-I Characteristics for 2 ternary (LS, STC) and 2 quarternary (S_2, LW) lasers. 50

Page

Figure 4.3: Variation of polynomial coefficients (a) A_o (b) A_1 (c) A_2 with temperature for L-V Characteristics for 2 ternary (LS, STC) and 2 quarternary (S_2 LW) lasers. 51

Figure 4.4: Variation of polynomial coefficients (a) A_3 (b) A_4 with temperature for L-V Characteristics for 2 ternary (LS, STC) and 2 quarternary (S_2, LW) lasers. 52

Figure 4.5: Variation of polynomial coefficients (a) A_o (b) A_1 (c) A_2 with temperature for I-V Characteristics for 2 ternary and 2 quarternary lasers. 53

Figure 4.6: Temperature vs natural log of drive current for various values of light output for (a) GaAlAs and (b) GaInAsP lasers. 56

CHAPTER 1

INTRODUCTION

The importance of semiconductor laser diodes in optical fibre communication[8] and research activities has led to the production of several types based on various conditions of low threshold current density, high peak power output, monomode operation and narrow beam width. Each laser design must be tested and testing involves spectral, spatial, thermal and electro-optical characteristics.

The objective of this work is to study the behaviour of lasers in the vicinity of the lasing threshold. This was done by fitting polynomial equations to the light-current (L-I), light-voltage (L-V) and current-voltage (I-V) characteristics curves of the lasers and investigating the relationships between the coefficients of the fitting polynomial and laser design parameters. Such relationships are expected to help in the design process since laser structures, compositions etc can then be simulated.

The work is based on the data acquired from an auto logger at UWIST[15]. This controller shown in figure 1.1b consists of a microprocessor automated system, which is used to control, measure and record the drive current, light output and voltage values for the diode at various temperatures. A typical sets of L-I, L-V and I-V curves for a GaAlAs ternary and a GaInAsP quarternary lasers are shown in figures 2.1 to 2.3.

These series of curves cannot be easily fitted by a single

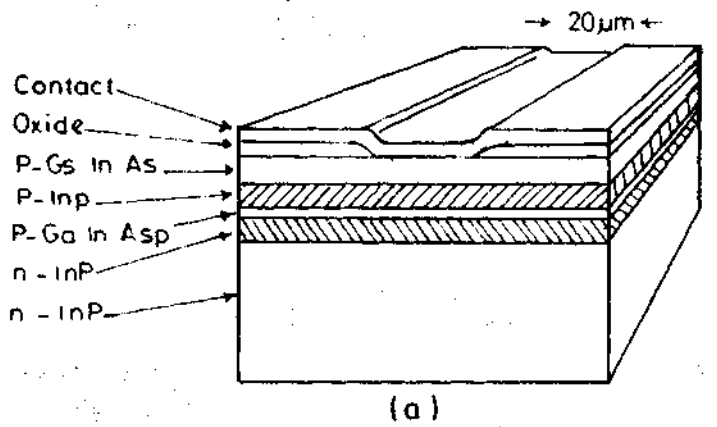

(a)

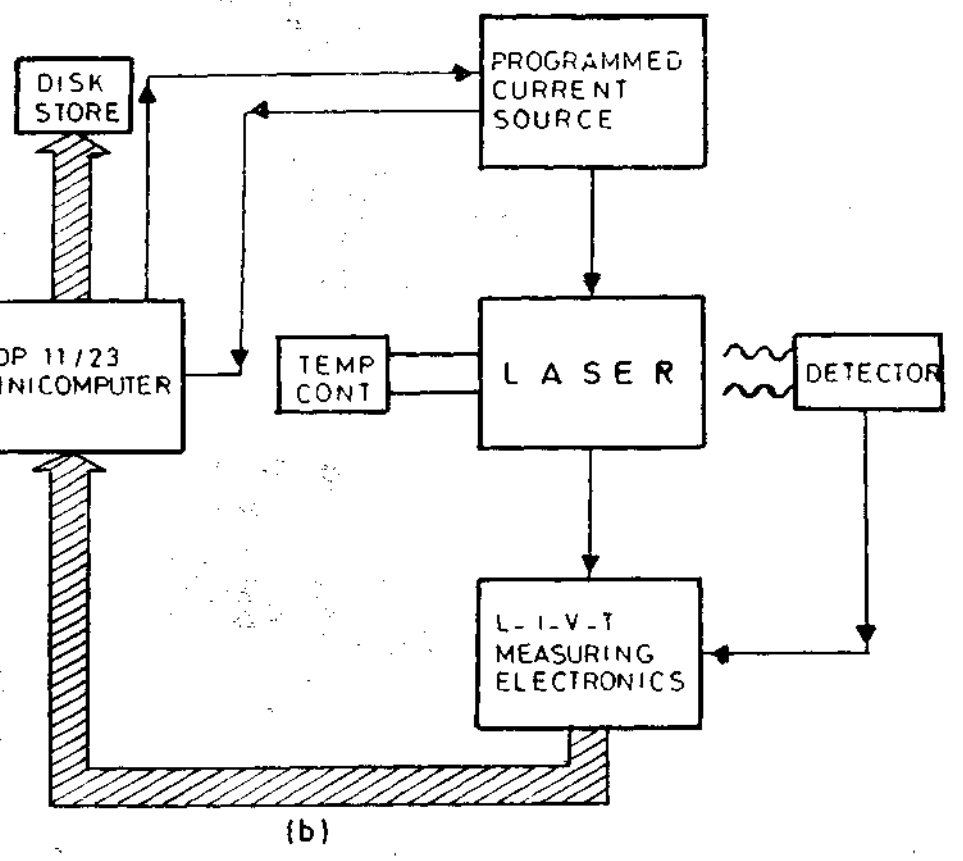

(b)

FIG 1.1: (a) InP/GaInAsP 20μm OXIDE STRIPE LASER (After Kirkby, ref-8)

(b) AUTOMATIC CW L-I-V-T MEASURENT OF A LASER (After Oyedokun, ref. 15)

equation because the coefficients of the fitting function vary with temperature. The fitting function can be written as

$$L = f\ (I, T) \qquad (1\text{-}1)$$

where f is the function which relates the light output to the current and temperature, L is the light output, I the current and T is the temperature.

For Isothermal conditions, the equation reduces to

$$L = g\ (I) \qquad (1\text{-}2)$$

where g is the new function which relates L to I at constant temperature.

The series of curves in figures 2.1 and 2.2 can be divided into three regions:

(i) spontaneous emission

(ii) the curve around the threshold and

(iii) stimulated emission region.

Both (i) and (iii) are essentially linear and can each be represented by the equation

$$L = A_o + A_1 I \qquad (1\text{-}3)$$

where the A's are the coefficients of the linear equation which will correctly fit each of these regions.

However, the threshold region is not linear and can therefore be represented for various Isothermal conditions by polynomial equation of the form

$$L = A_o + A_1 I + A_2 I^2 .... + A_n I^n \qquad (1\text{-}4)$$

where the A's are the coefficients of the polynomial which will correctly fit this region and n is the degree of the polynomial.

The task is to

(i) find n, the order of the polynomial that best fits the curve

(ii) establish goodness of fit

(iii) select correct points for the curve fitting and

(iv) interpret the coefficient values of the fitting polynomial in terms of laser design parameters.

The numerical analysis in Chapter 3 showed that a polynomial equation of order 4 will describe the threshold region for L-I and L-V characteristics. This can be accounted for in terms of the dependence of the light output on several parameters of the laser like active layer thickness, doping level, material composition, geometrical design etc. In the case of I-V characteristics, a polynomial equation of order 2 was found to fit the data accurately. This is expected because a well known simple relationship exists between current and voltage values for semiconductor laser diodes.

The coefficients of the fitted equations were also found to vary with temperature and the threshold current was found to be determinable from a combination of these coefficients. Also each of the coefficients exhibits a well defined variation with temperature and may be related to such other laser parameters as threshold voltage, junction resistance, active layer thickness, material composition etc. This is expected to aid laser design for different level of performance.

Further numerical analysis in Chapter 3 showed that another way of presenting laser characteristics can be derived from L-I characteristics. This characteristics called temperature-current characteristics (T-I) showed clearly the effect of current and temperature changes on the optical output of the laser and is hence expected to find applications in the design of temperature and current modulator for the laser. Also, the temperature sensitivity T_o of the laser can be calculated to a good approximation from the T-I characteristics.

For completeness, a review of physics of semiconductor lasers operation and their electro-optical characteristics are presented in Chapter 2, followed by the discussion and application of numerical analysis to laser electro-optical characteristics in Chapter 3. The discussion of the result obtained was presented in Chapter 4 and finally, the conclusion in Chapter 5.

CHAPTER 2

2. PRINCIPLE OF OPERATION OF SEMICONDUCTOR LASER DIODES AND THEIR ELECTRO-OPTICAL CHARACTERISTICS

2.1 General Considerations

The semiconductor laser diode is a sandwitch of two or more semiconductor materials which have different electrical properties. Like other forms of laser, it consists of an active medium which is a semiconductor from III/V family which are direct energy gap semiconductors. The parallel cleavage planes of these materials possess natural reflectivity which is used as an optical feedback to produce optical amplification.

An important part of semiconductors is their heterostructures.[3] These consists of layers of different materials having the same lattice constant but different band gap energies. In a conventional double heterostructure laser shown in figure 1.1a, the basic structure consists of three thin epitaxial single crystal layers grown on a single crystal substrate. The two thicker confining layers are wider gap materials which are doped p- and n- type.

When a forward current passed through the p-n junction becomes large, the density of electrons and holes in the active layer can become high enough to cause population inversion. At this point, a photon produced by a recombination event will trigger the emission of another photon having the same frequency and phase as the first. This is laser action and the current at which this occurs is the laser threshold current.

When the current is increased above this threshold value, light

emission (by radiative recombination of carriers) exceeds the losses due to absorption within the crystal cavity and light lost through the end mirrors. At this point, recombination is almost 100% efficient and the actual lasing starts. Along p-n junction, the radiation will resonate back and forth both in the transverse and longitudinal direction between the two crystal facet mirrors, stimulating further emission with each pass. In the end, an intense and highly directional laser beam will be emitted.

The current density required to reach the threshold is often very high, resulting in energy generation and heat dissipation[9], and thus making it difficult to operate the laser at high temperature. It is therefore necessary to confine both the carriers and the light output in both the transverse and longitudinal direction between the end mirrors.

2.2 Heterostructure Confinement

Mixed semiconductor materials are normally used for producing heterostructure lasers. Any change in composition of these materials produces a change in both the bandgap and the refractive index. Hence, it is possible to adjust the composition of the outer layers with respect to the central layer so that a potential barrier is created to confine the injected carriers and at the same time an optical waveguide is created by refractive index distributions to confine the light.

In GaInAsP quarternary double heterostructure (DH) laser shown in figure 1.1a, [8] three thin single crystal layers of

GaInAsP are grown on InP substrate since GaInAsP can be adjusted to have the same lattice constant as InP within a certain range.[7], [3] Similarly, in GaAlAs ternary double heterostructure laser, three thin epitaxial single crystal layers of GaAlAs are grown on a single crystal GaAs substrate. GaAlAs can be varied in composition over the entire range and can therefore be considered to have the same lattice constant as GaAs.[2], [3]

However, it is essential that a constant lattice match exists between the two semiconductor materials. If the lattice constant mismatch is considerable, dislocation are formed at the layer interface. These dislocations are undesirable as they always result in rapid non-radiative recombinations and higher thresholds.[13], [3] In GaAlAs/GaAs system, lattice match is easily achieved but in GaInAsP/InP system careful adjustment of the compositions of GaInAsP has to be made to minimise lattice mismatch.

In both GaAlAs and GaInAsP lasers, the wider bandgap of the passive layers form a potential well which prevents the diffusion of injected carriers out of the active region. Also, the refractive index in the confining layers is lower than in the active region and this results in the formation of a narrow waveguide which confines the light in the plane of the active layer as it propagates within the cavity.

However, the disadvantage of this narrow waveguide is that highly concentrated light interracts with surface states causing

catastrophic degradation of the end mirrors in the cavity and thereby limiting the possible optical output power of the laser.[7] This can be prevented by using the separate confinement method.[3], [23] In this method, a very much wider waveguide is grown with weaker refractive index steps to form a five-layer structure. This results in a more effective control of carrier leakage since there is an additional outer heterojunction. The active layer, also with slightly weaker refractive index steps is made narrower so that it does not confine the light and thus allow a wider optical distribution.

2.3 Lateral Confinement

The injected carriers and light output can be further confined in the lateral direction by making the electrical contact a narrow stripe and putting a cladding material of a different refractive index on each side of the active region to act as a lateral waveguide. This prevents the injected carriers from spreading into the region beneath the stripe and therefore lowers the threshold current. This confinement of laser activity in the lateral direction has resulted in several different types of designs and are known as stripe geometry lasers. [3], [18], [23] The lateral waveguide can be obtained by depositing silicon dioxide insulating layer on the top surface to form an oxide-defined stripe geometry laser, or by producing high resistivity regions either by proton bombardment or oxygen implantation on the two sides of the stripe.

In both the oxide stripe geometry and proton bombarded stripe lasers, carrier confinement or light guiding is not satisfac-

torily achieved because of lateral current spreading and diffusion of carriers out of the region beneath the stripe. However, carrier and optical confinement can be improved by deliberate confinement of light in the lateral direction. When there is deliberate lateral waveguide, then the lasers are classified as advanced laser structures.[8], [23] Three of these types of structures are the buried hetero-structure, transverse junction stripe and the rib-loaded stripe lasers. In the buried heterostructure stripe lasers, the change in composition of semi-conductor material is used to achieve lateral current and optical confinement. In the case of transverse junction stripe laser, a change in doping level causes the creation of one or more p-n junctions intersecting the active layer and provides a good means of injecting or confining electrons to the p-region. Also, the light is guided in the p- region by the virtue of dielectric constant difference. In the rib-loaded stripes, any increase in the thickness of the active layer or the adjacent passive layers causes an increase in the dielectric constant and hence is used for creating optical waveguide.

2.4 Feedback and Frequency Selection

Feedback for laser diode oscillator is provided by the natural reflectivity of the natural cleavage planes of the active layer of the chip. These parallel cleavage planes form a cavity called Fabry-Perot Cavity.[24] When the light resonates back and forth along the length of the cavity, only those frequencies at which an integral number of wavelength will fit between the two end mirrors will be positively reinforced. Other modes that

are produced which are not positively reinforced are called longitudinal modes. Similarly, in the transverse direction, only those resonances with half integral wavelength which will roughly fit across the transverse dimension are positively reinforced and are called fundamental transverse modes. Other frequencies having more than one peak (more than half wavelength) which are not reinforced are called higher order transverse modes and they have an effect of broadening the laser beam. Laser diodes which emit both the fundamental transverse mode and only one longitudinal mode are called single frequency lasers and are mostly used as signal sources in optical fibre communication.

It is however, essential to have a means of frequency selection in order to produce a good mode control. One method of achieving this is to set an external diffraction grating opposite one end facet of the laser. The wavelength of the radiation to be reinforced can be selected by tilting the grating at a suitable angle. Another method, which is presently favoured involves periodic variation of the refractive index within the waveguide by substituting the end mirrors with a grating, and suitably adjusting these gratings. When the period of this grating is equal to half integral wavelength of light output, Bragg's condition is satisfied and the light will be reflected exactly back and forth. Those frequencies that do not satisfy Bragg's condition are allowed to pass through with minimum loss. Lasers that utilises Bragg's condition are called Distributed Feedback (DFB) or Distributed Bragg Reflector (DBR) lasers[23], [25], [26] and their frequency selectivity helps to determine

the frequency.

2.5 Semiconductor Materials for Lasers

The semiconductor material used in the active layer are direct bandgap materials. These are materials which have spherical energy bands with the extrema occuring at the zero value of the crystal wave-vector k, and the transition of an electron across the bandgap Eg does not involve momentum change. In the indirect bandgap materials like Ge, Si and GaP where the conduction band minima are located at $k \neq o$, the combination of an electron at $k \neq o$ and a hole at $k = o$ will give rise to momentum change. Phonon participation is therefore required for conservation of momentum. Also, the life time of an electron in the indirect valley is relatively longer than in direct valley and thus there is higher probability of non-radiative recombination involving defects and impurities in the indirect bandgap materials. This explains why direct bandgap materials are used in semiconductor lasers.

There are many binary compounds such as GaAs which are direct bandgap and are hence used as semiconductor materials for lasers. The most important of these compounds are the III/V semiconductor materials which comprise of Al, Ga, and In in group III and P, As and Sb in group V. These binary compounds are used as substrates for epitaxial growth of structure layers on these substrates often involves composition grading in which the lattice constant of the heterostructure layers are adjusted to be almost the same as that of the substrate materials in order to attain lattice

match.[2] This is very important as lattice mismatch often gives rise to lattice defects recombination centres and dislocations which are highly undesirable. The most important ternary materials among the III/V semiconductors is the GaAlAs/GaAs system in which the lattice mismatch is very low. Other semiconductors materials of interest in the III/V family are GaInAsP/InP and (GaAl)(AsSb)/GaAs quarternary systems.[24] Those that have been successfully used for laser among the IV/VI compounds include Pb and Sn salts of Se and Te and their mixed solid solutions. Among the II/VI compounds only CdTe has been successfully used as a laser.[24]

The choice of lasers however depends on the wavelength that is required. For example, if short wavelengths are required, ternary lasers are the obvious choice but for long wavelength requirement, quarternary lasers are the best choice.

2.6 Electro-Optical Characteristics of Laser Diodes

The increased use of semiconductor lasers as signal sources in optical fibre communication[8] and in research activities has motivated a more detailed study of the characteristics of these lasers. For this purpose, a special project has been set up which uses an automated control and data acquisition system where the drive current, applied voltage and light output are measured at various temperatures and stored in the computer memory.

In this work, four lasers, two of which are GaAlAs ternary DH lasers and code named STC and LS and two of which are GaInAsP

quarternary DH lasers and code named S_2 and LW were analysed using numerical methods. The L-I, L-V and I-V characteristics for STC ternary and S_2 quarternary lasers are presented in figures 2.1 to 2.3 using the data acquired from automatic testing of laser diodes.[15]

Figures 2.1 and 2.2 showed that at lower values of drive current, the L-I and L-V characteristics are partly linear and correspond to spontaneous emission. When population inversion occurs in which the optical gain is equal to the optical loss, threshold current is reached. Above the threshold current, the optical gain exceeds optical loss and radiative recombination becomes almost 100% efficient. At this point, the linear portion of the curves corresponds to stimulated emission. In some lasers, most especially stripe geometry lasers, the L-I curve above threshold may not be linear because of formation of kinks. These kinks consists of points of inflexions which varies the near field distribution of the output. The formation of kinks can be reduced by suitably adjusting the width of the stripe and by improving the growth of the various heterostructure layers.

The threshold current can be determined by different methods which include:

(i) extrapolation of the linear portions of the spontaneous and stimulated emission region and the current at the intersection is the threshold current.

(ii) extrapolation of the stimulated emission region to

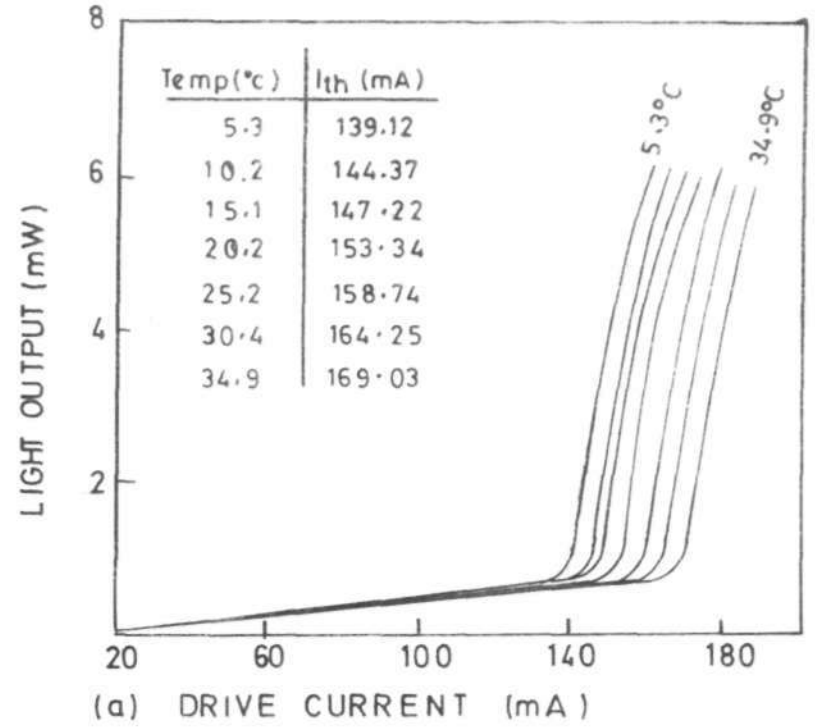

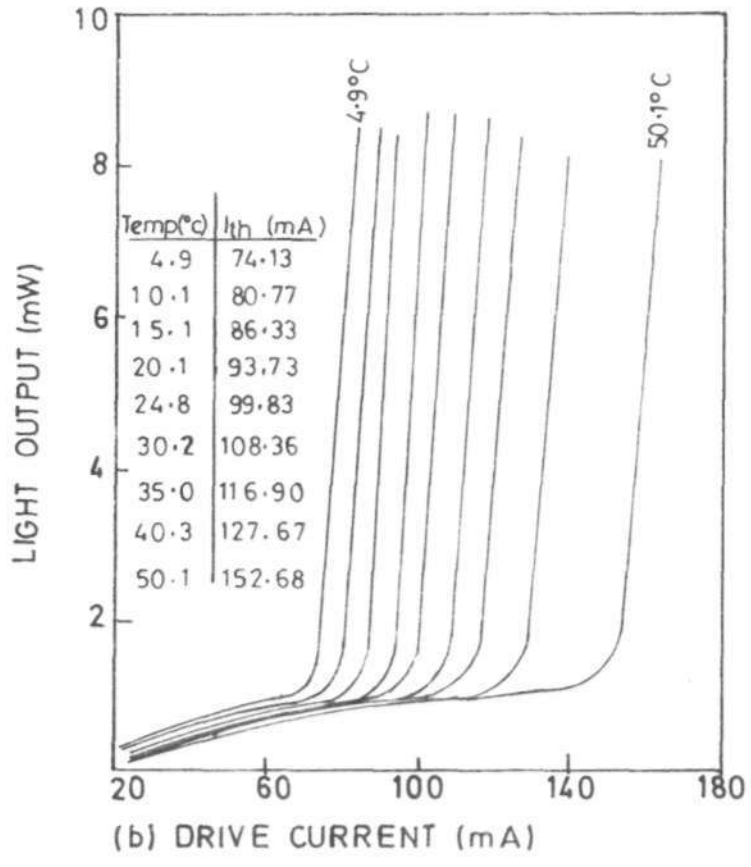

FIG. 2.1: LIGHT OUTPUT VS CURRENT CHARACTERISTICS FOR (a) GaAlAs AND (b) GaInAsP LASERS USING THE DATA ACQUIRED FROM AUTOMATIC TESTING OF LASER DIODE. THE INSERT SHOWS THE VARIATION OF THRESHOLD CURRENT WITH TEMPERATURE.

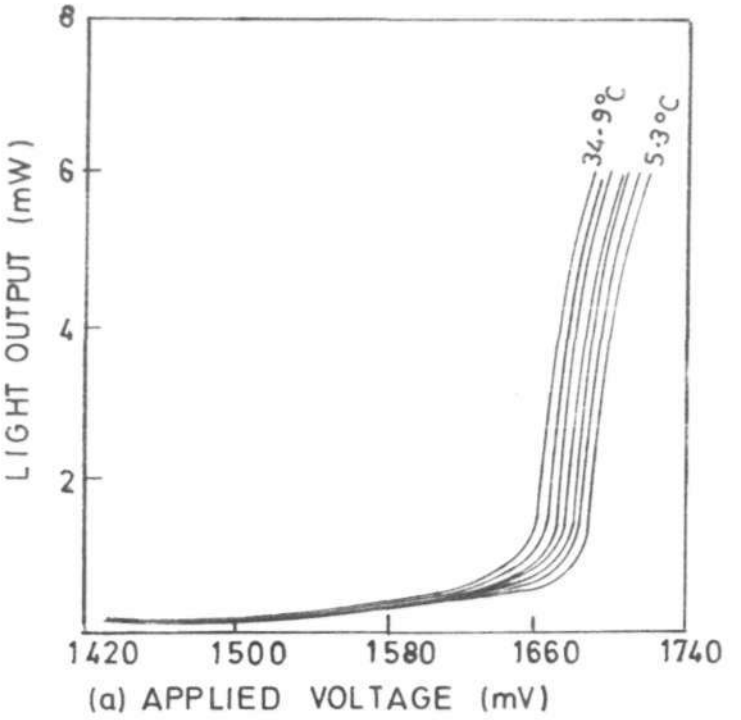

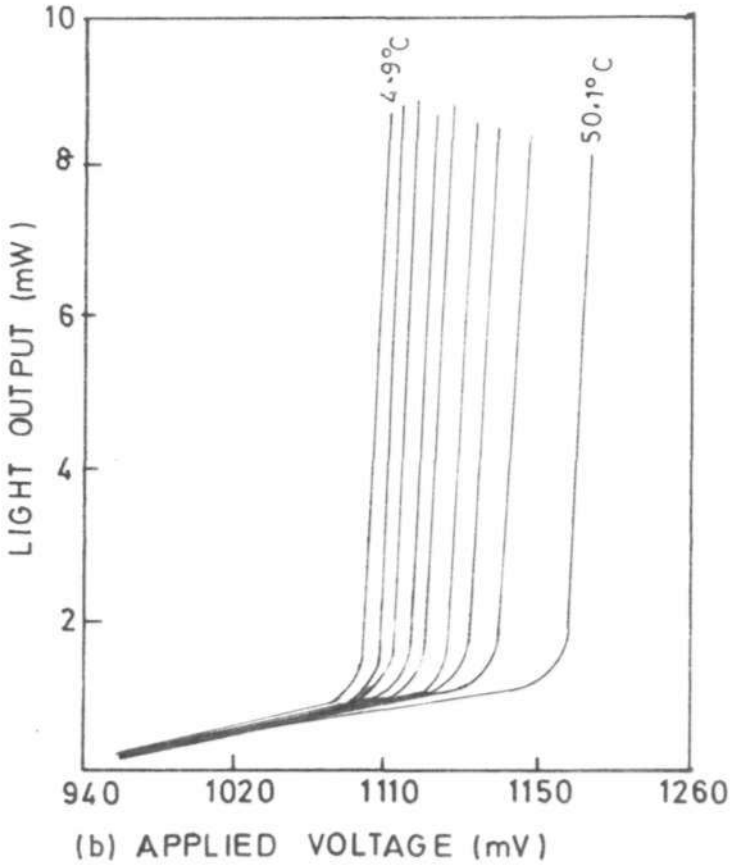

FIG 2.2: LIGHT OUTPUT VS VOLTAGE CHARACTERISTICS FOR (a) GaAlAs AND (b) GaInAsP LASERS USING THE DATA ACQUIRED FROM AUTOMATIC TESTING OF LASER DIODE.

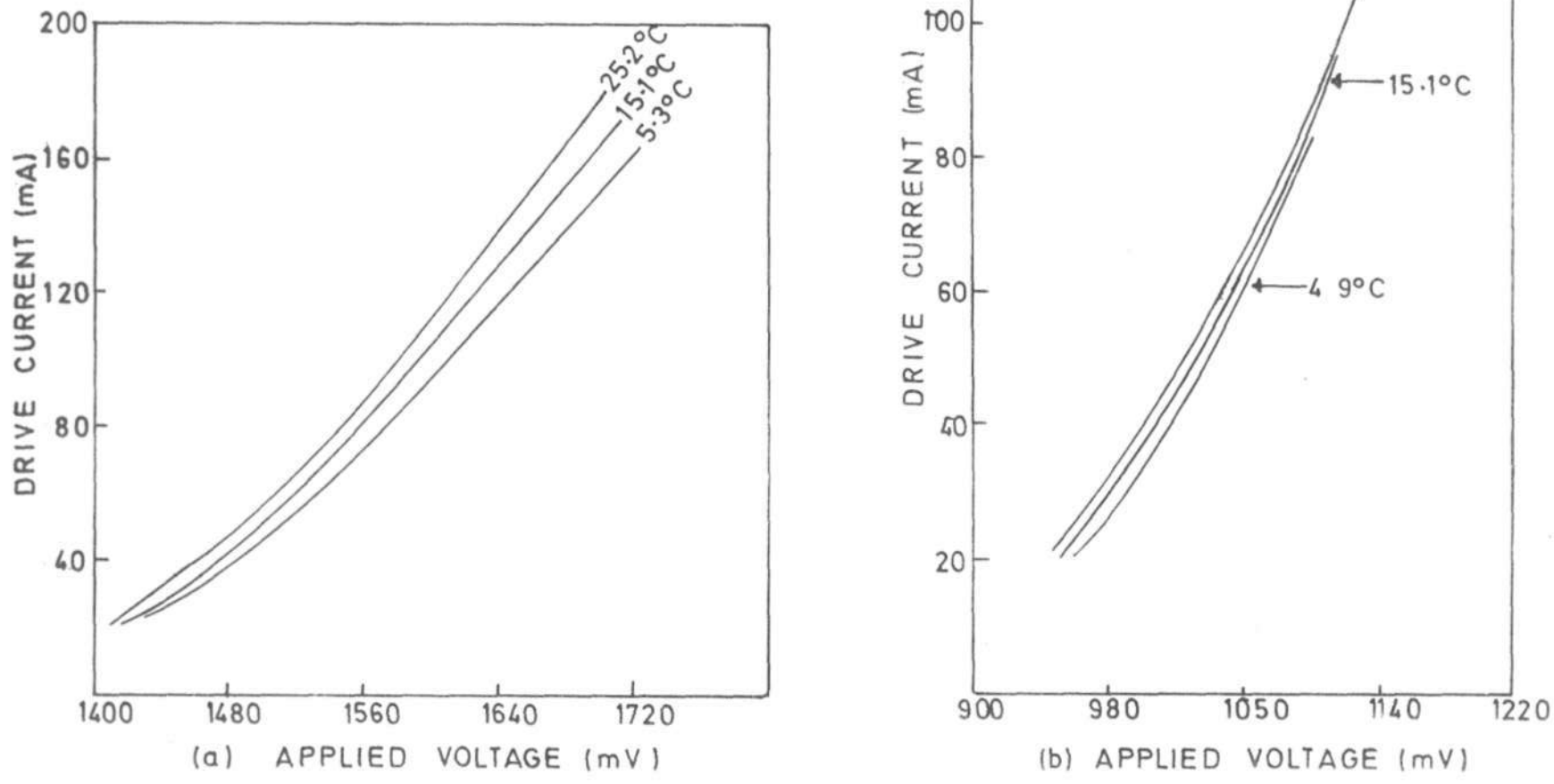

FIG 2·3: CURRENT VS VOLTAGE CHARACTERISTICS FOR (a) GaAlAs (STC)
(b) GaInAsP (S_2) LASERS.

zero light output. The value of current at zero light output is equal to threshold current provided there are no kinks.

(iii) Observing the highest peak in the graph of $\frac{d^2L}{dI^2}$ against I in which case the current corresponding to the peak value is equal to the threshold current.

The threshold current is affected by temperature changes. The inserted tables in figure 2.1 show the variation of threshold current with temperature for GaAlAs and GaInAsP lasers. The tables show that there is a more rapid increase in threshold current with temperature for the GaInAsP quarternary laser than for GaAlAs ternary laser and thus illustrates the major difference between the two lasers.

The threshold current of semiconductor lasers show an approximately exponential variation with temperature according to equation: [9]

$$I_{th} = I_o \exp (T/T_o) \qquad (2\text{-}1)$$

where I_{th} is the threshold current, T is the temperature of the heat sink on which the laser is mounted and T_o is the temperature sensitivity.

Between 0 and 70°C, T_o has a value of 100 - 180°C for GaAlAs and 50 - 80°C for GaInAsP lasers, thus showing that quarternary lasers are more sensitive to temperature changes than ternary lasers. [8]

The increase in threshold current with temperature can be attributed to energy spread of injected carriers across the conduction and valence bands. However, the much more rapid increase of I_{th} with temperature for quarternary laser appears to be a fundamental property of the laser and there had been a suggestion that it may be due to non-radiative recombination involving Auger process.[10]

Another striking difference between ternary and quarternary lasers can be seen in figure 2.2. The curves show that while the threshold voltage increases with increasing temperature for quarternary lasers, it decreases with temperature for ternary lasers.

CHAPTER 3

NUMERICAL ANALYSIS OF LASER DIODE ELECTRO-OPTICAL CHARACTERISTICS

3.1 Numerical Analysis of Experimental Data

Numerical analysis most often involves fitting a function to experimental data. Typically, when treating a set of data by numerical methods, errors can arise in two areas: those inherent in the mathematical formulation of the problem and those that arise in finding solution numerically. The former category includes the error incurred when the mathematical statement of the problem only approximates the physical situation and they are often negligible. The latter category involves inaccuracies in the physical and experimental data. In the case of physical data the error is also negligible but for experimental data, the errors may be considerable. Other sources of errors include gross error, truncation error and round-off error. However, one of the aims of numerical analysis is to smoothen out these errors.

Most of the problems often encountered involves fitting a function to a set of points (X_i, Y_i), i = 1, 2, ... n which approximates them as closely as possible. The type of functions often considered are the polynomial and cubic splines. The degree of the polynomial and the number of knots (the x-values of points at which the cubic polynomials are joined together) in the cubic spline determine the order of the fitting function.

In fitting experimental data, both the smoothness and closeness requirement is achieved by restricting the degree of the

polynomial or the number of knots in a spline, while the closeness requirement is achieved by ensuring that the deviation of the approximating function from the data points is as small as possible.

A measure of distance between the fitting function and data can be achieved by summing the squares of the difference between the experimental and theoretical points.

i.e $$(Y_i - f(X_i))^2 = \sum_{i=1}^{N} e_i^2 \qquad (3\text{-}1)$$

where Y_i represents experimental data, e_i is the error and $f(X_i)$ is the fitting function. This leads to the least squares fit. It is however assumed that the random errors in Y_i are independent of one another and that errors in X_i are relatively negligible.

In this work, the least squares polynomial fit was used because the curves represented by the experimental data are simple curves and the errors incurred in choosing the optimum number of coefficients can easily be found by calculating the variance of theoretical points with respect to experimental points.

3.2 Polynomial Representation of the Electro-optical Characteristics of the Laser Diode

The sets of L-I and L-V curves in figures 2.1 and 2.2 can be zoned into three parts:

(i) The spontaneous emission region which is partly linear

(ii) The threshold region

(iii) The stimulated emission region which is essentially

linear.

The fitted region consists of parts of spontaneous and stimulated region in addition to the threshold region and for various isothermal conditions may be represented by a polynomial equation of the form

$$L = f(I) = A_o + A_1 I + A_2 I^2 + ... A_n I^n \qquad (3\text{-}2)$$

where L is the light output, I is the current , n is the degree of the approximating polynomial required to fit each curve, and the A's are the coefficients of the fitting polynomial.

3.2.1 Theory of Polynomial Curve-fitting by least squares Method

The vicinity of the lasing threshold may be represented for Isothermal conditions by the polynomial equation

$$f(x) = A_o + A_1 X + A_2 X^2 + ... + A_n X^n \qquad (3\text{-}3)$$

To obtain an equation of the above nature by numerical technique, polynomial curve-fitting by least squares method is used to fit the characteristics data obtained from integrated automatic tester. In this method Y_i represents experimental values and $f(x_i)$ represents the value obtained from the fitting equation. Then equation (3-3) becomes

$$f(X_i) = A_o + A_1 X_i + A_2 X_i^2 + ...+ A_n X_i^n \qquad (3\text{-}4)$$

where X_i is a particular value assumed free of error.

The best values of the coefficients A_1 to A_n of the function $f(X_i)$ that fits the data correctly can be determined by

calculating the error e_i between the experimental value Y_i and the theoretical value $f(X_i)$.

The least squares fit requires that for N values of X, Y, pairs

$$s = \sum (Y_i - A_o - A_1X_i - A_2X_i^2 - .... A_nX_i^n)^2 = \sum e_i^2 \qquad (3\text{-}6)$$

must be a minimum.

i.e $\delta s/\delta A_o$, $\delta s/\delta A_1$ ..... $\delta s/\delta A_n$ must be equal to zero. This leads to n+1 equations:

$$\frac{\delta s}{\delta A_o} = o = \sum 2(Y_i - A_o - A_1X_i - ..... -A_nX_i^n)\ (-1)$$

$$\frac{\delta s}{\delta A_1} = o = \sum 2(Y_i - A_o -A_1X_i - ..... - A_nX_i^n\ )\ (-X_i)$$

$$\vdots \qquad\qquad \vdots$$

$$\frac{\delta s}{\delta A_n} = o = \sum 2(Y_i - A_o - A_1X_i - ..... -A_nX_i^n)\quad (-X_i^n) \qquad (3\text{-}7)$$

Dividing by - 2 and re-arranging, we have

$$A_oN + A_1 \sum X_i + A_2 \sum X_i^2 + ...+ A_n \sum X_i^n = \sum Y_i$$

$$A_o \sum X_i + A_1 \sum X_i^2 + ...+ A_n \sum X_i^{n+1} = \sum X_iY_i$$

$$\vdots \qquad\qquad\qquad\qquad\qquad\qquad \vdots$$

$$A_o \sum X_i^n + A_1 \sum X_i^{n+1} .....+ A_n \sum X_i^{2n} = \sum X_i^nY_i \qquad (3\text{-}8)$$

The n+1 equations in equation (3-8) can be arranged in a matrix form as

$$\begin{bmatrix} N & \sum X_i & \sum X_i^2 \cdots & \sum X_i^n \\ \sum X_i & \sum X_i^2 & \sum X_i^3 \cdots & \sum X_i^{n+1} \\ \sum X_i^2 & \sum X_i^3 & \sum X_i^4 \cdots & \sum X_i^{n+2} \\ \vdots & & & \\ \sum X_i^n & \sum X_i^{n+1} & \sum X_i^{n+2} \cdots & \sum X_i^{2n} \end{bmatrix} A = \begin{bmatrix} \sum Y_i \\ \sum X_i Y_i \\ \sum X_i^2 Y_i \\ \vdots \\ \sum X_i^n Y_i \end{bmatrix} \quad \ldots\ldots (3\text{-}9)$$

where all the summations in equations (3-7) to (3-9) runs from 1 to N.

However, the round off errors in solving these equations simultaneously cause unusually large errors when the degree of the approximating polynomial is greater than 5.

3.2.2 Application of Polynomial Curve-fitting to Laser Electro-Optical Characteristics

When the computer program designed for solving equation (3-9) was applied to the characteristics curves shown in figures 2.1 to 2.3, it was found that the fitting function approximates the curve to reasonable accuracy when a small region in the vicinity of lasing threshold was fitted and when the current was used as dependent variable. In fitting the curves, the following steps were taken:

(i) The fitted regions in L-I, L-V and I-V characteristics included parts of the spontaneous and stimulated emission region

in addition to the threshold region. Also, the same region was fitted for all the characteristics at all temperatures for a particular laser since the coefficients of the fitting function vary with temperature and curve.

(ii) The chosen degree of polynomial was determined by calculating the variance of the theoretical points with respect to experimental points which must be a minimum. For both L-I and L-V characteristics, polynomial of degree 4 gives minimum value of variance while degree 2 gives the minimum value of variance for I-V characteristics.

Using the data for light output, drive current and applied voltage from the automatic tester in the computer program designed for solving equation (3-9), the coefficients of the fitted equations at various temperatures for L-I, L-V and I-V characteristics were obtained for all the lasers. The variance of each fitted curve with respect to experimental values were also calculated. These are presented in tables 3.1 to 3.3 shown below.

Table 3.1: Variation of the coefficients of the fitting polynomial with temperature for L-I characteristics for (a) GaAlAs (STC) laser (b) GaAlAs (LS) laser (c) GaInAsP (S_2) laser (d) GaInAsP (LW) laser.

Temperature (K)	A_o	A_1	A_2	A_3	A_4	Variance
298.3	-33.245	530.852	-586.697	278.522	-47.961	0.40
283.2	-33.112	540.857	-593.483	279.364	-47.655	0.38
288.1	-31.358	542.962	-587.797	272.648	-45.805	0.42
293.2	-31.959	556.675	-599.830	277.587	-46.601	0.40
298.2	-31.025	561.508	-596.340	272.055	-45.038	0.42
303.4	-30.420	568.504	-596.999	268.804	-43.865	0.41
307.9	-30.450	579.960	-602.912	268.869	-43.471	0.42

(a)

Temperature (K)	A_o	A_1	A_2	A_3	A_4	Variance
278.1	-50.236	830.694	-1187.242	731.235	-163.805	0.40
283.1	-48.621	834.791	-1175.069	711.812	156.731	0.39
288.2	-46.781	836.982	-1156.168	687.347	-148.520	0.41
293.2	-44.205	846.792	-1164.613	690.587	-148.974	0.38
298.2	-46.105	859.699	-1154.491	667.823	-140.372	0.35

(b)

Temperature (K)	A_o	A_1	A_2	A_3	A_4	Variance
277.9	-88.964	338.950	-247.981	76.394	-8.397	1.09
283.1	-93.504	352.860	-252.055	75.891	-8.172	1.29
288.1	-115.042	411.828	-297.318	90.558	-9.863	0.87
293.1	-135.604	465.373	-336.653	103.438	-11.416	1.34
297.8	-158.654	526.784	-381.578	116.990	-12.844	0.79
303.2	-158.715	531.107	-375.179	112.281	-12.061	1.08
308.0	-179.247	587.287	-415.122	124.509	-13.413	1.11
313.3	-197.761	636.811	-446.145	133.166	-14.314	1.40
323.1	-243.635	755.409	-518.268	152.215	-16.161	2.32

(c)

Temperature (K)	A_o	A_1	A_2	A_3	A_4	Variance
278.1	- 62.534	255.740	-147.473	37.771	- 3.581	0.08
283.3	- 59.573	252.606	-137.953	33.405	- 2.996	0.04
288.1	- 83.094	308.151	-172.853	42.881	- 3.934	0.07
293.2	-106.915	368.416	-213.513	54.650	- 5.167	0.06
298.1	-123.069	410.864	-239.298	61.484	- 5.830	0.11
303.3	-106.635	386.820	-215.105	52.666	- 4.750	0.10
308.1	-151.835	487.396	-279.613	70.636	- 6.586	0.20
313.2	-171.177	539.805	-309.206	77.966	- 7.247	0.25

(d)

Table 3.2: Variation of the coefficients of the fitting polynomial with temperature for L-V Characteristics for (a) GaAlAs (STC) laser (b) GaAlAs (LS) Laser (c) GaInAsP (S_2) laser (d) GaInAsP (LW) laser

Temperature (K)	A_o	A_1	A_2	A_3	A_4	Variance
278.3	1367.095	1009.803	-1156.644	569.020	-101.453	0.75
283.2	1365.291	997.777	-1136.557	555.298	- 98.225	0.69
288.1	1367.862	966.001	-1082.049	519.562	- 90.384	0.64
293.2	1363.275	973.287	-1093.567	528.877	- 92.854	0.58
298.2	1363.932	953.982	-1053.968	500.994	- 86.473	0.56
303.4	1359.745	959.139	-1051.784	495.701	- 84.883	0.56
307.9	1358.257	956.529	-1041.502	488.956	- 83.567	0.58

(a)

Temperature (K)	A_o	A_1	A_2	A_3	A_4	Variance
278.1	1343.706	1509.479	-2258.756	1455.998	-340.813	0.51
283.1	1345.076	1446.465	-2134.179	1355.678	-312.862	0.46
288.2	1346.115	1384.263	-2011.949	1260.996	-287.501	0.50
293.2	1352.491	1322.102	-1980.452	1189.631	-270.019	0.32
298.2	1344.702	1309.791	-1863.062	1147.406	-257.928	0.30

(b)

Temperature (K)	A_o	A_1	A_2	A_3	A_4	Variance
277.9	752.026	703.110	-516.644	159.332	-17.509	1.99
283.1	742.038	728.823	-527.695	160.663	-17.469	2.02
288.1	709.961	813.436	-592.008	181.303	-19.826	1.57
293.1	688.522	861.978	-619.928	188.707	-20.612	4.77
297.8	639.449	989.453	-719.396	220.724	-24.214	0.82
303.2	642.394	986.425	-702.652	211.658	-22.860	1.37
308.0	607.634	1078.021	-768.769	232.108	-25.135	1.41
313.3	583.925	1137.764	-801.379	239.823	-25.806	1.58
323.1	510.121	1322.500	-915.976	270.875	-28.909	1.36

(c)

Temperature (K)	A_o	A_1	A_2	A_3	A_4	Variance
278.1	812.967	490.296	-290.526	76.193	-7.378	0.36
283.3	824.146	463.834	-258.716	63.708	-5.797	0.19
288.1	786.079	549.485	-315.384	79.903	-7.476	0.18
293.2	754.439	626.441	-367.963	95.336	-9.118	0.18
298.1	732.936	678.646	-398.721	103.127	-9.830	0.27
303.3	749.927	653.735	-372.203	93.212	-8.600	0.10
308.1	684.589	796.287	-465.877	119.911	-11.381	0.43
313.2	661.623	857.776	-500.042	128.181	-12.107	0.43

(d)

Table 3.3: Variation of the coefficients of the fitting polynomial with temperature for I-V Characteristics for (a) GaAlAs (STC) laser (b) GaAlAs (LS) Laser (c) GaInAsP (S_2) laser (d) GaInAsP (LW) laser.

Temperature (K)	A_o	A_1	A_2	Variance
278.3	1407.014	2.3607	-0.0026	0.04
283.2	1403.715	2.2794	-0.0025	0.04
288.1	1400.694	2.2048	-0.0023	0.04
293.2	1399.291	2.1092	-0.0020	0.04
298.2	1394.813	2.0802	-0.0020	0.04
303.4	1388.094	2.0798	-0.0020	0.05
307.9	1389.180	1.9706	-0.0017	0.04

(a)

Temperature (K)	A_o	A_1	A_2	Variance
278.1	1402.150	2.3696	-0.0028	0.04
283.1	1398.753	2.2343	-0.0025	0.04
288.2	1395.148	2.1048	-0.0022	0.04
293.2	1392.429	2.0058	-0.0020	0.08
298.2	1388.180	1.9229	-0.0019	0.04

(b)

Temperature (K)	A_o	A_1	A_2	Variance
277.9	887.1738	3.7106	-0.0136	0.08
283.1	891.4113	3.3959	-0.0106	0.03
288.1	899.2747	3.0430	-0.0078	0.04
293.1	907.7703	2.7168	-0.0056	0.05
297.8	912.0547	2.5137	-0.0041	0.04
303.2	910.7378	2.4649	-0.0038	0.05
308.0	912.1783	2.3595	-0.0031	0.03
313.3	912.8244	2.2803	-0.0027	0.03
323.1	912.4386	2.1566	-0.0020	0.03

(c)

Temperature (K)	A_o	A_1	A_2	Variance
278.1	909.3577	2.4898	-0.0042	0.06
283.3	910.5280	2.3691	-0.0035	0.03
288.1	913.9809	2.1940	-0.0026	0.04
293.2	917.3940	2.0530	-0.0019	0.05
298.1	919.4576	1.9486	-0.0015	0.05
303.3	904.5814	2.1800	-0.0021	0.05
308.1	915.0526	1.8924	-0.0013	0.03
313.2	912.4277	1.8794	-0.0013	0.05

(d)

In order to ascertain that the equations fit the experimental data to reasonable accuracy, the values of current Ic were regenerated from the fitted equations using the experimental values of light output Le. These theoretical values were compared with experimental values Ie in tables 3.4 and 3.5 for L-I, characteristics for GaInAsP (S_2) at 10.1^{o}C and GaAlAs (STC) at 10.2^{o}C. The tables show that the percentage differences between experimental and theoretical values are extremely low. The experimental and theoretical values are also compared graphically in figure 3.1 for L-I characteristics. The graphs show that most of the theoretical points coincide with experimental points except for 1 or 2 points. For I-V characteristics, the variance of theoretical points are so small that all the theoretical values are almost equal to experimental values.

Table 3.4: Comparison of experimental light-current characteristics data with calculated values for GaAlAs at 10.2°C. The calculated values of d^2L/dI^2 are also shown.

Le (mW)	Ie (mA)	Ic (mA)	% difference	$d^2L/dI^2(W^2/A^2)$
0.300	83.44	82.89	0.66	0.011
0.317	87.76	87.12	0.73	0.012
0.329	90.28	89.98	0.33	0.013
0.340	92.74	92.52	0.24	0.013
0.352	95.17	95.19	0.02	0.014
0.370	98.84	99.01	0.18	0.015
0.390	102.56	103.02	0.45	0.017
0.416	107.44	107.86	0.39	0.019
0.461	114.82	115.31	0.43	0.023
0.477	117.28	117.70	0.36	0.025
0.495	119.74	120.22	0.40	0.027
0.520	123.39	123.45	0.05	0.031
0.540	125.82	125.83	0.01	0.034
0.559	128.26	127.92	0.27	0.038
0.607	133.23	132.53	0.53	0.051
0.650	136.06	135.91	0.69	0.067
0.691	139.34	138.55	0.57	0.090
0.719	140.56	140.06	0.36	0.112
0.762	141.78	141.96	0.13	0.162
0.860	142.99	144.71	1.20	0.483
1.110	144.21	145.73	1.05	1.333
1.482	145.41	144.39	0.69	1.330
1.852	146.64	146.91	0.18	1.106

Table 3.5: Comparison of experimental light-current characteristics values with calculated values for GaInAsP laser at 10.1°C. The calculated values of d^2L/dI^2 are also shown.

Le (mW)	Ie (mA)	Ic (mA)	% Difference	d^2L/dI^2 (W^2/A^2)
0.700	53.65	53.97	0.60	0.023
0.789	61.32	62.02	1.14	0.032
0.855	66.71	66.99	0.43	0.041
0.886	69.17	69.02	0.21	0.046
0.922	71.68	71.16	0.72	0.054
0.942	72.93	72.25	0.93	0.059
0.964	74.14	73.37	1.03	0.065
0.988	75.28	74.56	0.96	0.073
1.017	76.58	75.77	1.05	0.084
1.061	77.82	77.45	0.47	0.107
1.132	79.04	79.63	0.75	0.165
1.332	80.27	80.92	0.81	1.152
1.979	81.40	80.46	1.15	0.352
2.907	82.71	83.28	0.69	0.152
3.400	83.35	83.23	0.14	0.391

Further justification of the goodness of fit was carried out by generating the values of d^2L/dI^2 from the fitting equation. The variation of d^2L/dI^2 with the drive current I, for GaInAsP at 10.1°C and for GaAlAs at 10.2°C are also presented in tables 3.4 to 3.5 and figure 3.2. The graphs show that d^2L/dI^2 increases steadily with temperature up to a maximum value

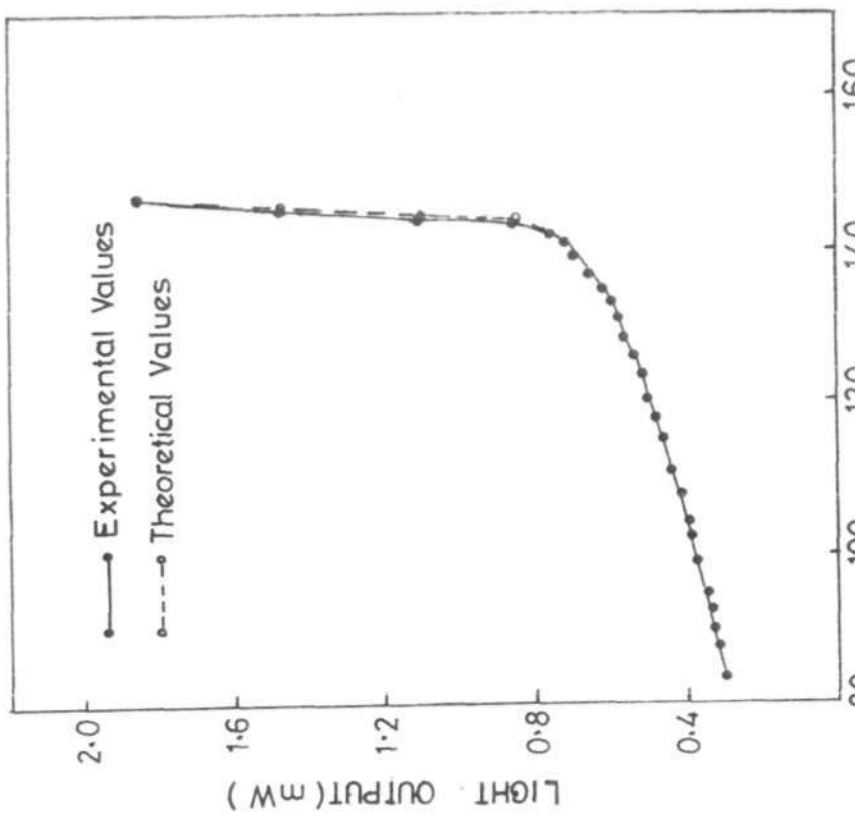

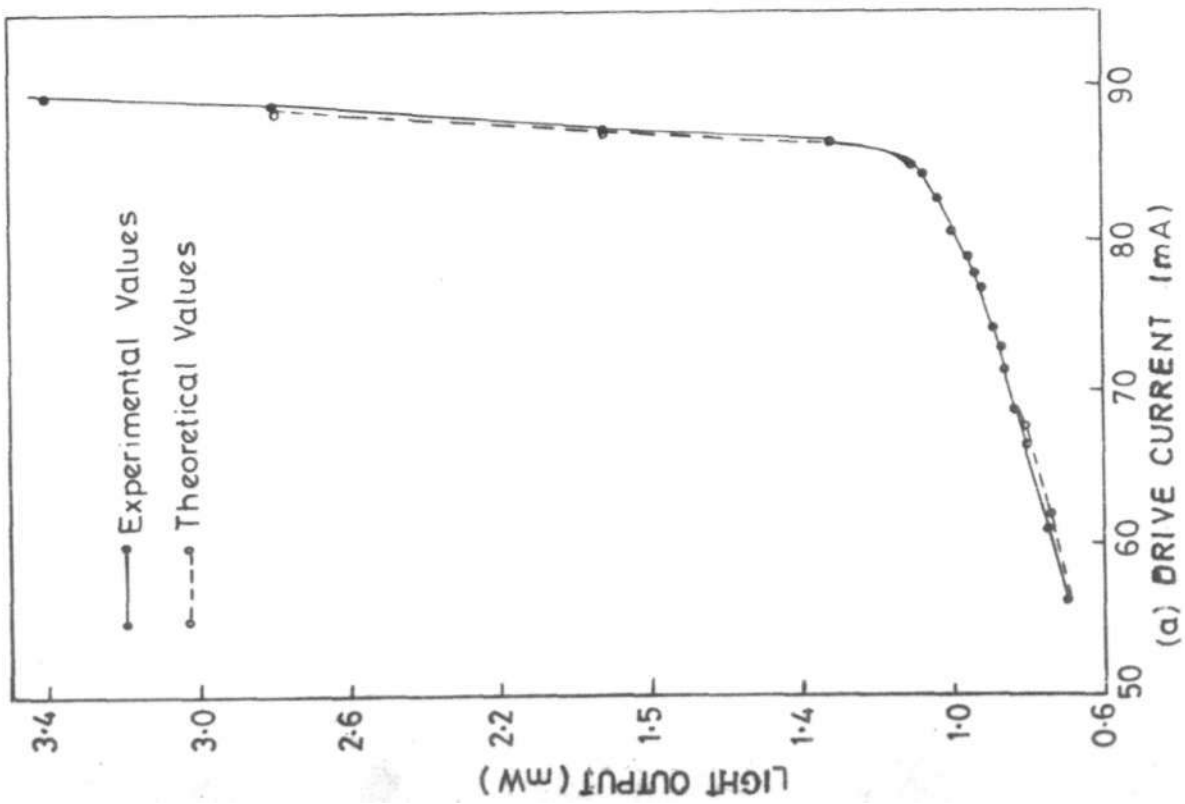

FIG 3.1: COMPARISON OF EXPERIMENTAL AND THEORETICAL VALUES FOR L-I CHARACTERISTICS FOR (a) GaInAsP DH LASER AT 10.1°C AND (b) GaAlAs DH LASER AT 10.2°C .

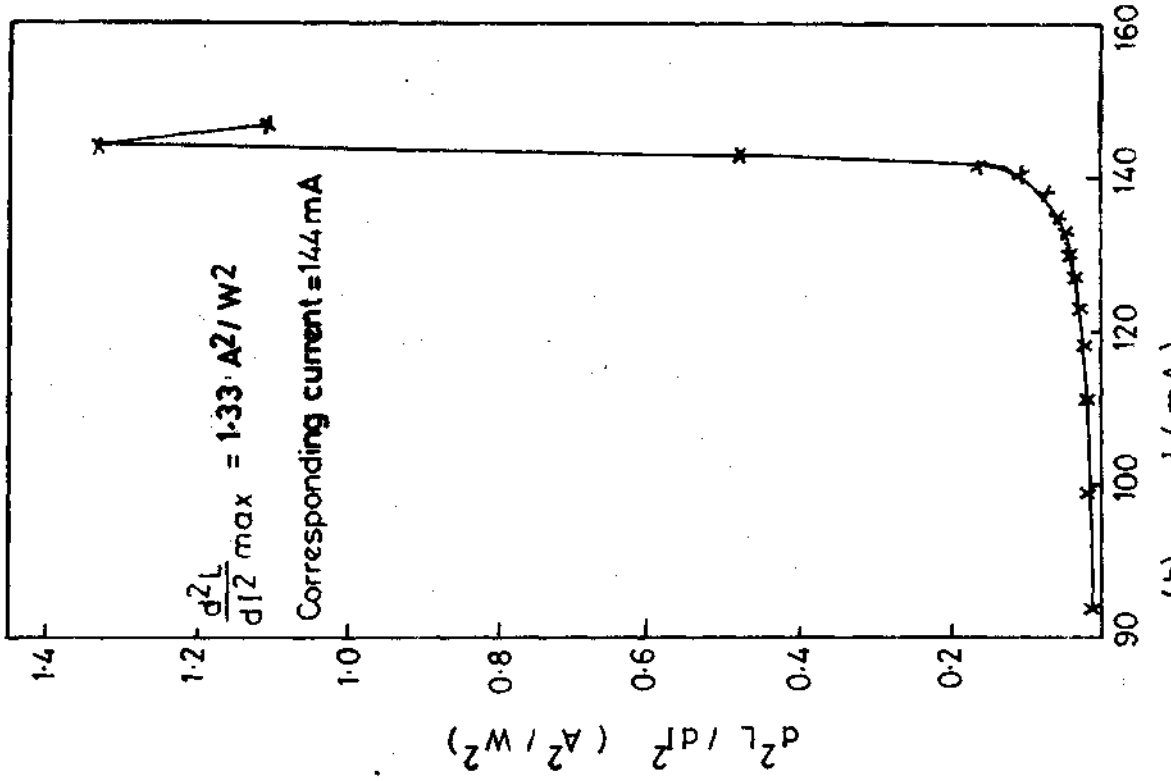

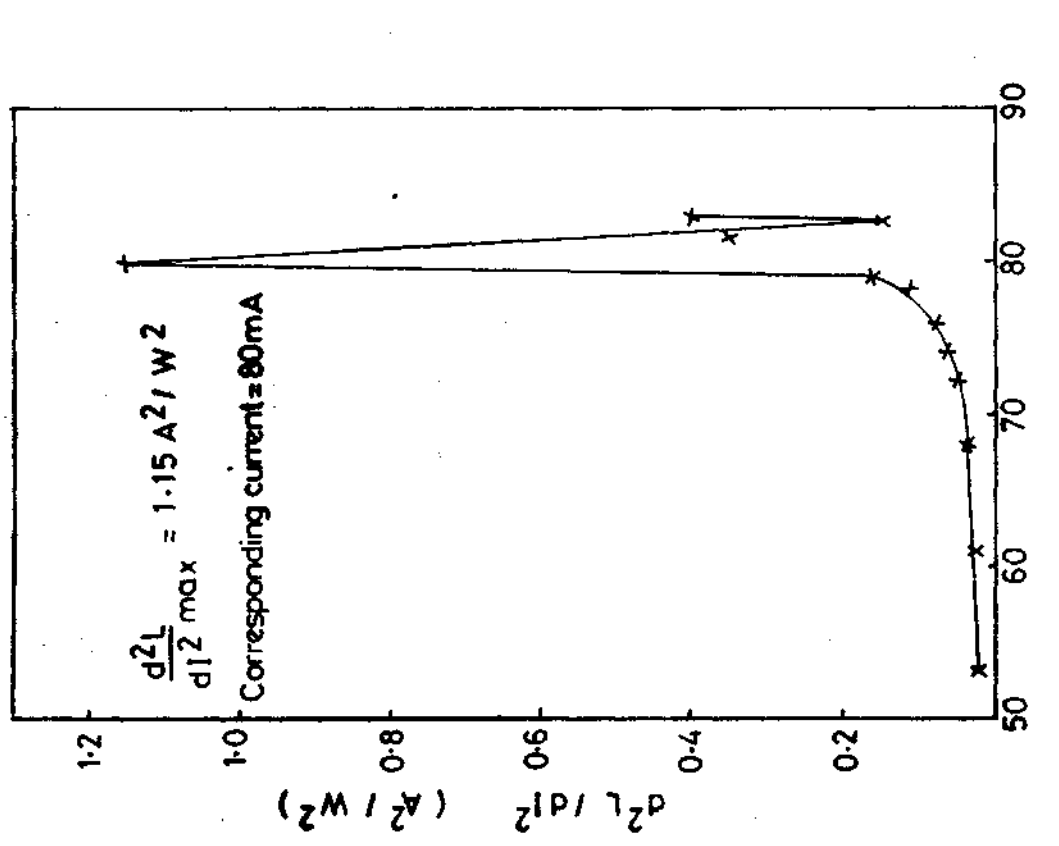

FIG 3·2:VARIATION OF d^2L/dI^2 WITH THE DRIVE CURRENT FOR (a) GaInAsP LASER AT 10·1°C AND (b.) GaAlAs LASER AT 10·2°C.

after which it starts decreasing. The value of the drive current corresponding to the highest peak of this graph for GaAlAs is 140 mA and for GaInAsP is 74 mA. These two values are approximtely equal to the threshold current of the lasers. It is therefore confirmed that the fitted equations fit the experimental data to reasonably high accuracy.

Tables 3.1 to 3.4 show that the coefficients of all the fitted equations vary with temperature for all the lasers. It is thus expected that a relationship exists between these coefficients and temperature dependent parameters of the laser.

3.3 Deduction of Temperature-current Characteristics from L-I Characteristics by Linear Interpolation

As mentioned in Chapter 3, for various isothermal conditions, the light output may be expressed in terms of current by the equation.

$$L = f\ (I) \qquad (3\text{-}10)$$

If the temperature is not constant, then equation (3-10) becomes

$$L = g\ (I, T) \qquad (3\text{-}11)$$

At constant optical output, equation (3-11) reduces to

$$T = g'\ (I) \qquad (3\text{-}12)$$

where g' is the function which relates temperature to current at constant light output. The relation (3-12) can be generated from L-I characteristics. This shows a new method of presenting laser characteristics.

The same program used for solving equation (3-9) was used to fit linear equations between two appropriate consecutive values of L-I characteristics data in which fixed values of light output had been interpolated. The corresponding current were then obtained from the fitted equation. This is repeated for all the temperature values. For each interpolated value of light output, values of current and temperature were recorded to obtain temperature-current (T-I) characteristics data. These are presented in Tables 3.6 and 3.7 for GaAlAs ternary and GaInAsP quarternary lasers.

The plots of T-I characteristics for various values of light output are also presented in figure 3.3 for a GaAlAs and a GaInAsP lasers to illustrate the result obtained for various laser diodes. The curves show exponential increase of current with temperature for both lasers. The curves in fig 3.3 (a) also show that if GaAlAs laser is operated above threshold, and the current is kept constant at about 150 mA, a small change in temperature of about 1.8 K (i.e from 282.2K to 284K) causes a shift from light output locus of 3.0 mW to locus of 2.5 mW, corresponding to about 17% decrease in light output. Similarly, for GaInAsP laser, fig 3.3 (b) shows that if the current is kept constant at 110 mA, an equal increase in temperature of about 1.8k (i.e from 300.4K to 302.2 K) causes a shift of light output locus from 5.0 mW to 3.0 mW corresponding to about 40% decrease in light output. This again confirms the higher temperature sensitivity of quarternary lasers compared to ternary lasers.

The effect of current changes on the optical output can also be

Table 3.6: Temperature-current Characteristics Data for GaAlAs ternary lasers

Light (mW)	LS		STC	
	Temperature (K)	Current (mA)	Temperature (K)	Current(mA)
0.5	278.1	150.18	278.3	117.09
	283.1	154.96	283.2	120.50
	288.2	160.00	288.1	124.22
	293.3	165.65	293.2	127.96
	298.2	170.42	298.2	131.47
	-	-	303.4	135.04
	-	-	307.9	139.28
1.0	278.1	160.82	278.3	139.26
	283.1	166.08	283.2	143.67
	288.2	172.53	288.1	148.14
	293.3	179.29	293.2	153.50
	298.2	186.19	298.2	158.77
	-	-	303.4	163.37
	-	-	307.9	169.37
1.5	278.1	162.99	278.3	140.98
	283.1	168.35	283.2	145.47
	288.2	174.95	288.1	149.91
	293.3	181.91	293.2	155.29
	298.2	188.78	298.2	160.57
	-	-	303.4	165.27
	-	-	307.9	171.31
2.0	278.1	165.38	278.3	142.61
	283.1	170.86	283.2	147.14
	288.2	177.64	288.1	151.56
	293.3	184.73	293.2	156.96
	298.2	191.48	298.2	162.22
	-	-	303.4	166.96
	-	-	307.9	173.01

Light (mW)	LS		STC	
	Temperature (K)	Current (mA)	Temperature (K)	Current(mA)
2.5	278.1	168.13	278.3	144.43
	283.1	173.68	283.2	148.90
	288.2	180.61	288.1	153.33
	293.3	187.88	293.2	158.72
	298.2	194.55	298.2	163.96
	-	-	303.4	168.73
	-	-	307.9	174.13
3.0	278.1	171.28	278.3	146.36
	283.1	176.94	283.2	150.75
	288.2	183.93	288.1	155.24
	293.3	191.23	293.2	160.64
	298.2	197.93	298.2	166.14
	-	-	303.4	170.61
	-	-	307.9	176.58

Table 3.7: Temperature-Current Characteristics data for GaInAsP Quarternary Lasers

Light (mW)	LW		S_2	
	Temperature (K)	Current (mA)	Temperature(K)	Current(mA)
0.5	278.1	42.67	277.8	34.60
	283.3	44.99	283.1	36.27
	288.1	47.37	288.1	37.98
	293.2	49.93	293.1	38.99
	298.1	52.63	297.8	40.54
	303.3	56.44	303.2	43.57
	308.1	58.75	308.0	45.54
	313.2	62.74	313.3	47.89
	-	-	323.1	52.74
1.0	278.1	79.86	277.9	70.68
	283.3	85.03	283.1	75.88
	288.1	90.97	288.1	80.94
	293.2	97.30	293.1	86.15
	298.1	103.98	297.8	91.58
	303.3	112.94	303.2	98.50
	308.1	119.73	308.0	105.02
	313.2	129.33	313.3	112.71
	-	-	323.1	130.28
1.5	278.1	98.66	277.9	74.66
	283.3	102.84	283.1	80.57
	288.1	115.26	288.1	86.68
	293.2	123.79	293.1	93.42
	298.1	133.14	297.8	100.14
	303.3	143.70	303.2	108.41
	308.1	155.61	308.0	116.77
	313.2	169.70	313.3	127.46
	-	-	323.1	151.83
2.0	278.1	103.78	277.9	75.56
	283.3	110.91	283.1	81.53
	288.1	121.49	288.1	87.65

Light (mW)	LW		S_2	
	Temperature (K)	Current (mA)	Temperature(K)	Current(mA)
2.0	293.2	130.08	293.1	94.40
	298.1	139.67	297.8	101.20
	303.3	151.02	303.2	109.48
	308.1	163.64	308.0	117.97
	313.2	178.49	313.3	128.81
	-	-	323.1	153.64
3.0	278.1	107.10	277.9	76.84
	283.3	116.00	283.1	82.83
	288.1	124.81	288.1	89.01
	293.2	133.63	293.1	95.84
	298.1	143.52	297.8	102.64
	303.3	155.42	303.2	110.97
	308.1	167.59	308.0	119.56
	313.2	183.61	313.3	130.53
	-	-	323.1	155.58
5.0	278.1	110.20	277.9	79.38
	283.3	120.78	283.1	85.45
	288.1	129.78	288.1	91.66
	293.2	139.28	293.1	98.54
	298.1	149.46	297.8	105.40
	303.3	162.31	303.2	113.83
	308.1	174.60	308.0	122.54
	313.2	192.24	313.3	133.65
	-	-	323.1	158.97

investigated by keeping the temperature constant. The sets of curves in figure 7 show that if the laser is operated above the threshold at constant temperature, very small changes in current result in significant changes in the optical output. For example, for GaAlAs laser at temperature of about 300K, a small change in current from about 140 mA to 143 mA, causes a shift from light output locus of 1.0 mW to 2.0 mW corresponding to about 50% increase in optical output. Similarly for GaInAsP laser at temperature of 300K, an equal change in current from about 74 mA to about 77 mA causes a shift from light output locus of 1.5 mW to 3.0 mW also corresponding to about 50% increase in optical output.

This characteristics is therefore expected to find application in the design of both current and temperature modulator for semiconductor lasers.

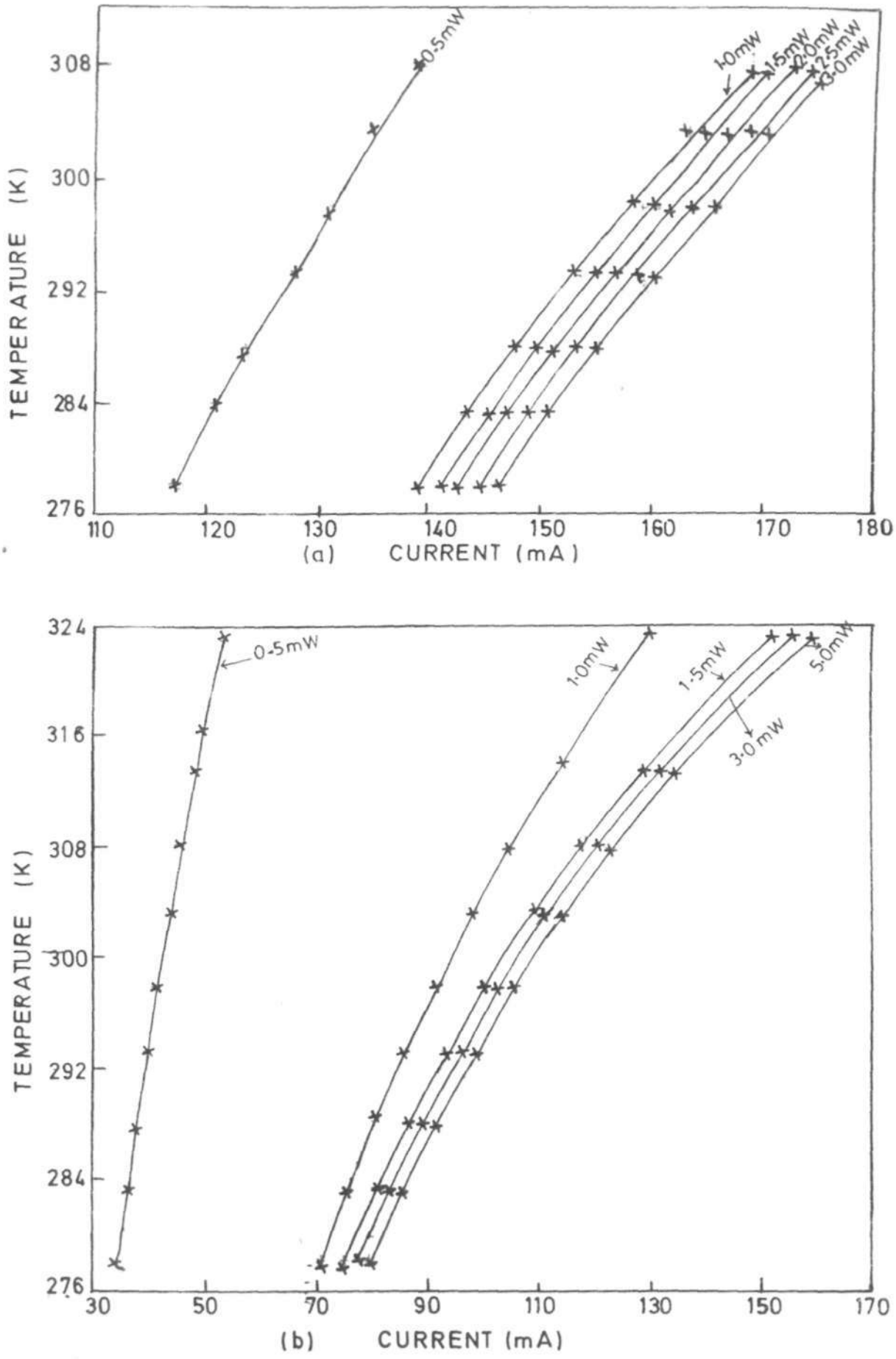

FIG 3·3: VARIATION OF TEMPERATURE WITH DRIVE CURRENT FOR VARIOUS VALUES OF LIGHT OUTPUT FOR (a) GaAlAs TERNARY LASER AND (b) GaInAsP QUARTERNARY LASER

CHAPTER 4

RESULTS AND DISCUSSION

In the previous chapter, it was shown that the electro-optical characteristics of a laser may be fitted with a polynomial equation at any particular temperature. The coefficients of these fits show remarkable variation with temperature. It is therefore expected that a relationship exists between these coefficients, temperature dependent parameters of the laser and the material composition and design of the laser.

Further analysis of L-I characteristics show that another characteristics in form of temperature-current characteristics can be derived. This characteristics clearly show the effect of temperature and current on the optical output of the laser and can therefore be used in designing temperature and current modulator for the laser. Further, the temperature sensitivity T_o can be calculated approximately from this characteristics.

4.2 Determination of Threshold Current from the Coefficients of the Fitting Polynomial

In Chapter 3, it was shown that the value of current corresponding to the maximum value of d^2L/dI^2 is approximately equal to the threshold current, using the graph in figure 3.2. From this graph, it is evident that the third derivative of light output with respect to current be equal to zero at the peak where the curve has a turning point. Hence, the threshold current can be calculated by evaluating d^3I/dL^3 using the fitting function, equating it to zero and substituting the then calculated value of light output back into the fitting function to obtain the threshold current.

For example, for GaInAsP (S_2) laser at 4.9°C, the fitting function is

$$I = - 88.964 + 338.95L - 247.98\ L^2 + 76.39\ L^3 - 8.397\ L^4 \qquad (4\text{-}1)$$

$$\frac{d^3I}{dL^3} = 3 \times 2 \times 76.394 - 4 \times 3 \times 2 \times 8.397\ L = 0 \qquad (4\text{-}2)$$

$$\text{i.e} \qquad L = \frac{3 \times 2 \times 76.394}{4x3x2 \times 8.397} = \frac{76.394}{4x8.397}$$

$$= - \frac{A_3}{4A_4} = 2.274\ \text{mW} \qquad (4\text{-}3)$$

$$I_{th} = - 88.964 + 338.95\ (2.274) - 247.98\ (2.274)^2 + 76.394\ (2.274)^3 - 8.397\ (2.274)^4 \qquad (4\text{-}4)$$

$$I_{th} = 73.26\ \text{mA} \qquad (4\text{-}5)$$

i.e., the threshold current is 73.26 mA which is approximately equal to the experimental value of 74.13 mA.

It can therefore be generalised that for any laser at any particular temperature, the threshold current I_{th} is, using equation (4-3), given by

$$I_{th} = A_o \frac{-A_1 A_3}{4A_4} + A_2 \left(\frac{A_3}{4A_4}\right)^2 - A_3 \left(\frac{A_3}{4A_4}\right)^3 + A_4 \left(\frac{A_3}{4A_4}\right)^4 \qquad (4\text{-}6)$$

where A_o, A_1, A_2, A_3 and A_4 are the coefficients of the fitting polynomial at the temperature concerned.

It can therefore be concluded that a relationship exists between the threshold current and the coefficients of the fitting function at a particular temperature as seen in figure 3.2 and equation (4-6). Table 4.1 below compares the value of threshold current calculated from equation (4-6), (Itc) with experimental values, Ite for GaInAsP and GaAlAs lasers at various temperatures.

Table 4.1: Comparison of calculated value of threshold current from equation (4-6) with experimental values at various temperatures for (a) GaInAsP and (b) GaAlAs lasers.

Temperature (K)	Ite (mA)	Itc (mA)	% difference
277.9	74.13	73.26	1.17
283.1	80.27	79.39	1.10
288.1	86.33	85.16	1.36
293.2	93.73	92.85	0.93
297.8	99.83	98.33	1.50
303.2	108.36	106.76	1.48
308.0	116.90	115.09	1.55
313.3	127.67	126.51	0.91
323.1	152.68	152.00	0.45

Temperature (K)	Ite (mA)	Itc (mA)	% difference
278.3	139.12	140.06	0.68
283.2	142.99	144.37	0.97
288.1	147.22	148.83	1.09
293.2	153.34	154.36	0.67
298.2	158.71	159.66	0.60
303.4	162.91	164.25	0.82
307.9	169.03	170.31	0.75

(b)

4.3 Variation of Coefficients A_i of the fitting Polynomial with Temperature

The tables of coefficients of the fitting polynomial in Chapter 3 show that each of the coefficients varies with temperature. The variation of the coefficients with temperature for L-I, L-V and I-V characteristics are presented in figures 4.1 to 4.5. The scales are unified so that the variation of each coefficient with temperature for all the lasers can be compared. All the graphs generally show that the variation of the coefficients with temperature for GaAlAs is generally small compared to that of GaInAsP lasers, again showing the higher temperature sensitivity of GaInAsP quarternary lasers. The behaviour of the coefficients for L-I, L-V and I-V characteristics is summarised below.

4.3.1 Variation of Polynomial Coefficients with temperature for L-I Characteristics

The variation of the coefficients of the fitting equation with temperature for this characteristics are presented in figures

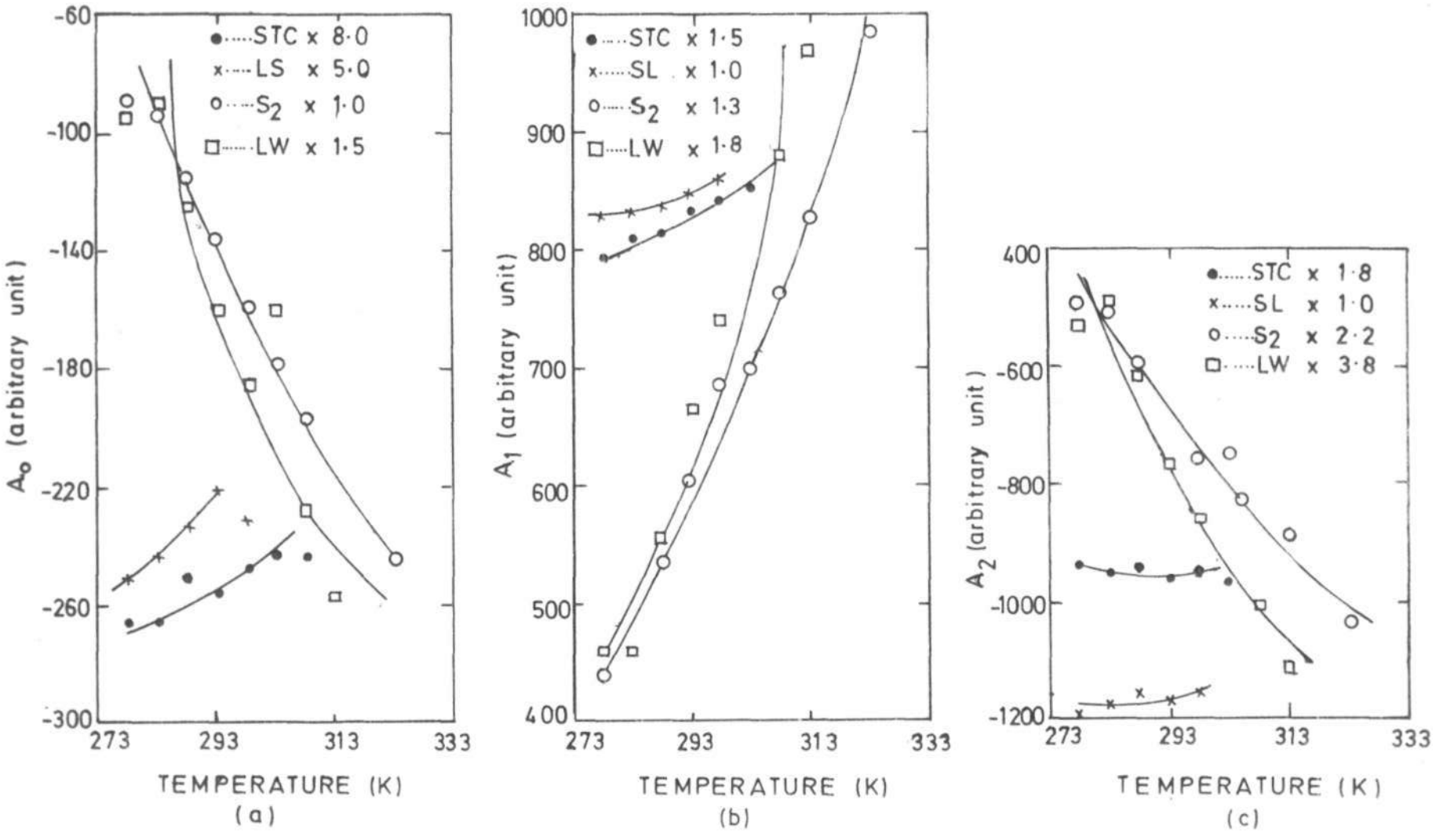

FIG 4.1: VARIATION OF POLYNOMIAL COEFFICIENTS (a) A_o, (b) A_1, (c) A_2 WITH TEMPERATURE FOR L-I CHARACTERISTICS FOR 2 TERNARY (LS, STC) AND 2 QUARTERNARY (S_2, LW) LASERS.

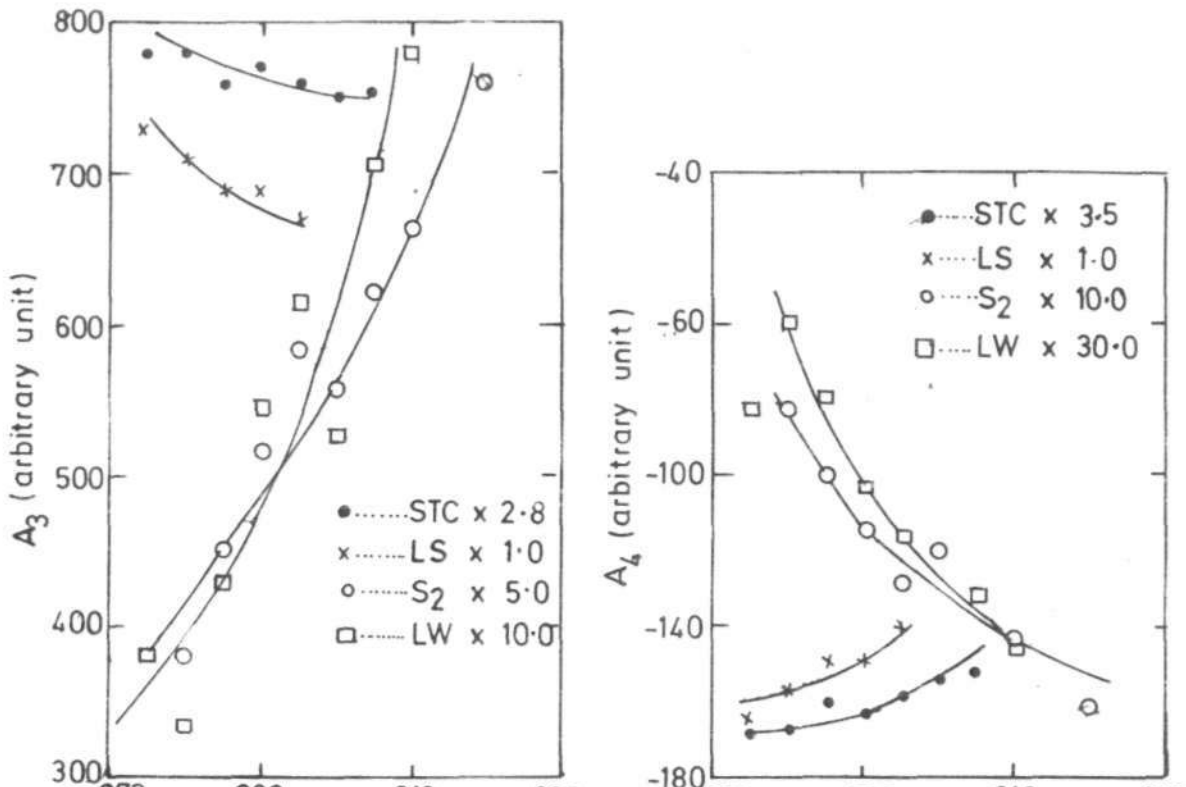

FIG 4·2: VARIATION OF POLYMOMIAL COEFFICIENTS (a) A_3, (b) A_4 WITH TEMPERATURE FOR L-I CHARACTERISTICS FOR 2 TERNARY (LS, STC) AND 2 QUARTERNARY (S_2, LW) LASERS.

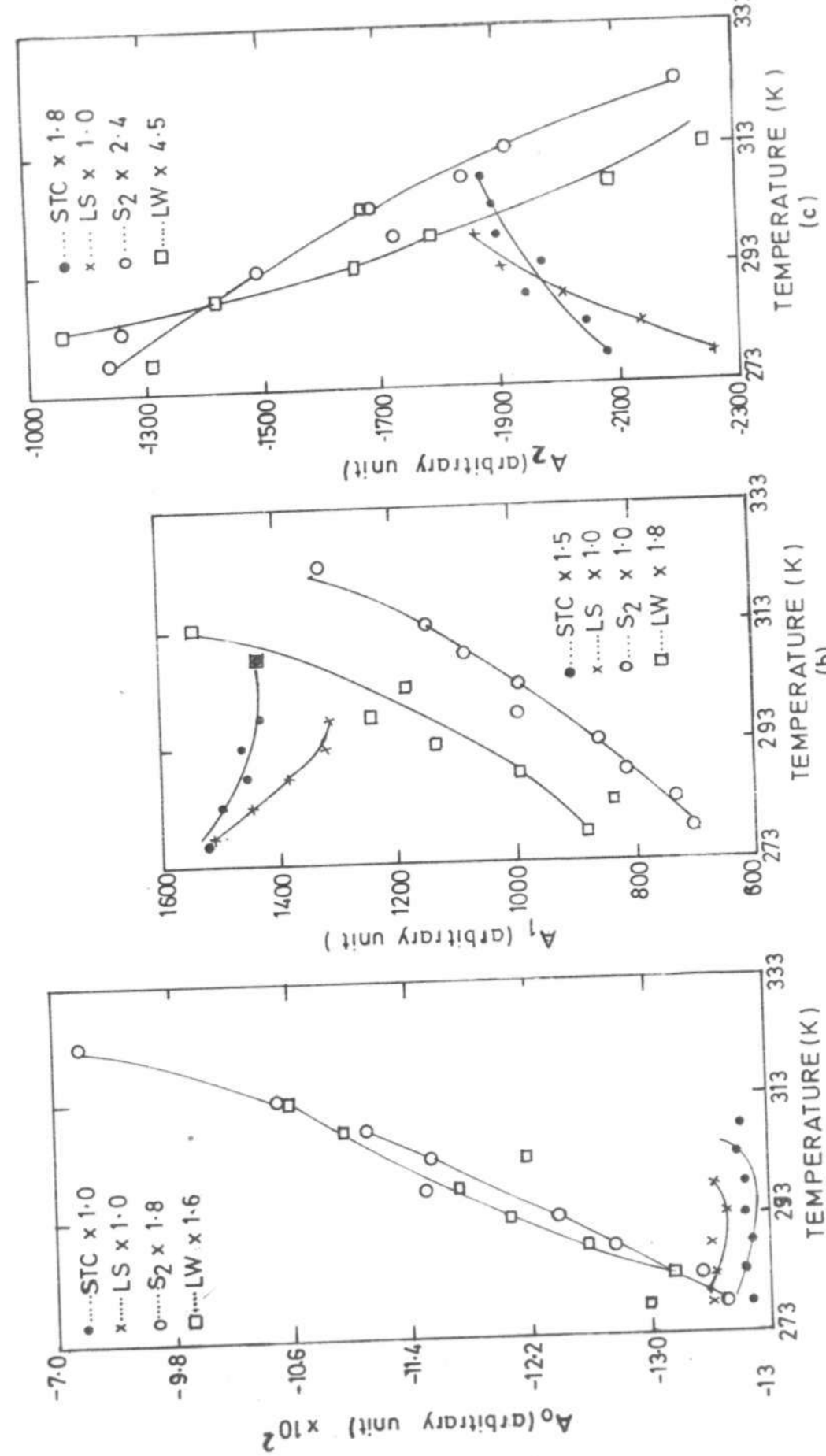

FIG 4·3: VARIATION OF POLYNOMIAL COEFFICIENTS (a) A_1, (b) A_2, (c) A_3 WITH TEMPERATURE FOR L-V CHARACTERISTICS FOR 2 TERNARY (LS, STC) AND 2 QUARTERNARY (S_2, LW) LASERS.

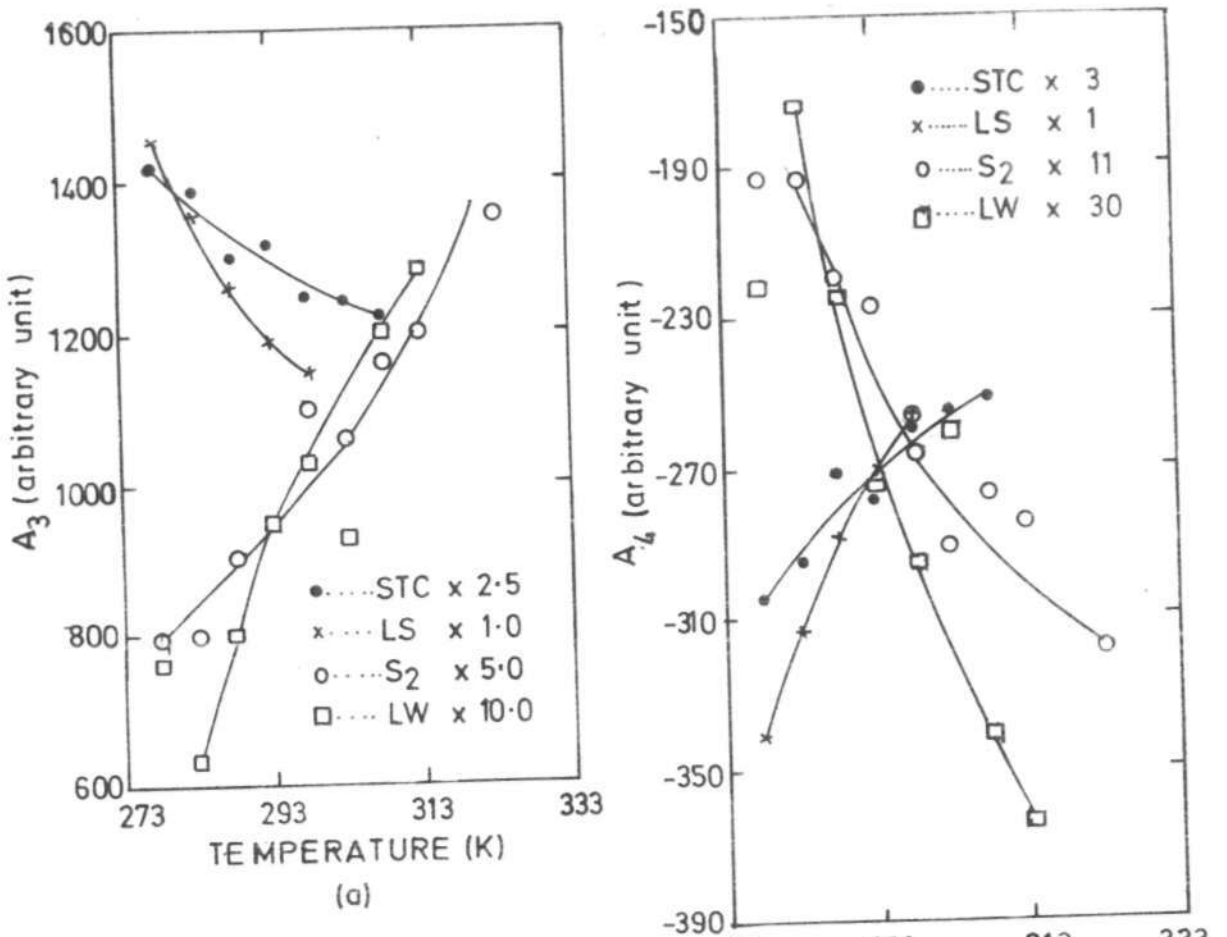

FIG 4.4: VARIATION OF POLYNOMIAL COEFFICIENTS (a) A_3 (b) A_4 WITH TEMPERATURE FOR L-V CHARACTERISTICS FOR 2 TERNARY (LS, STC) AND 2 QUARTERNARY (S_2, LW) LASERS.

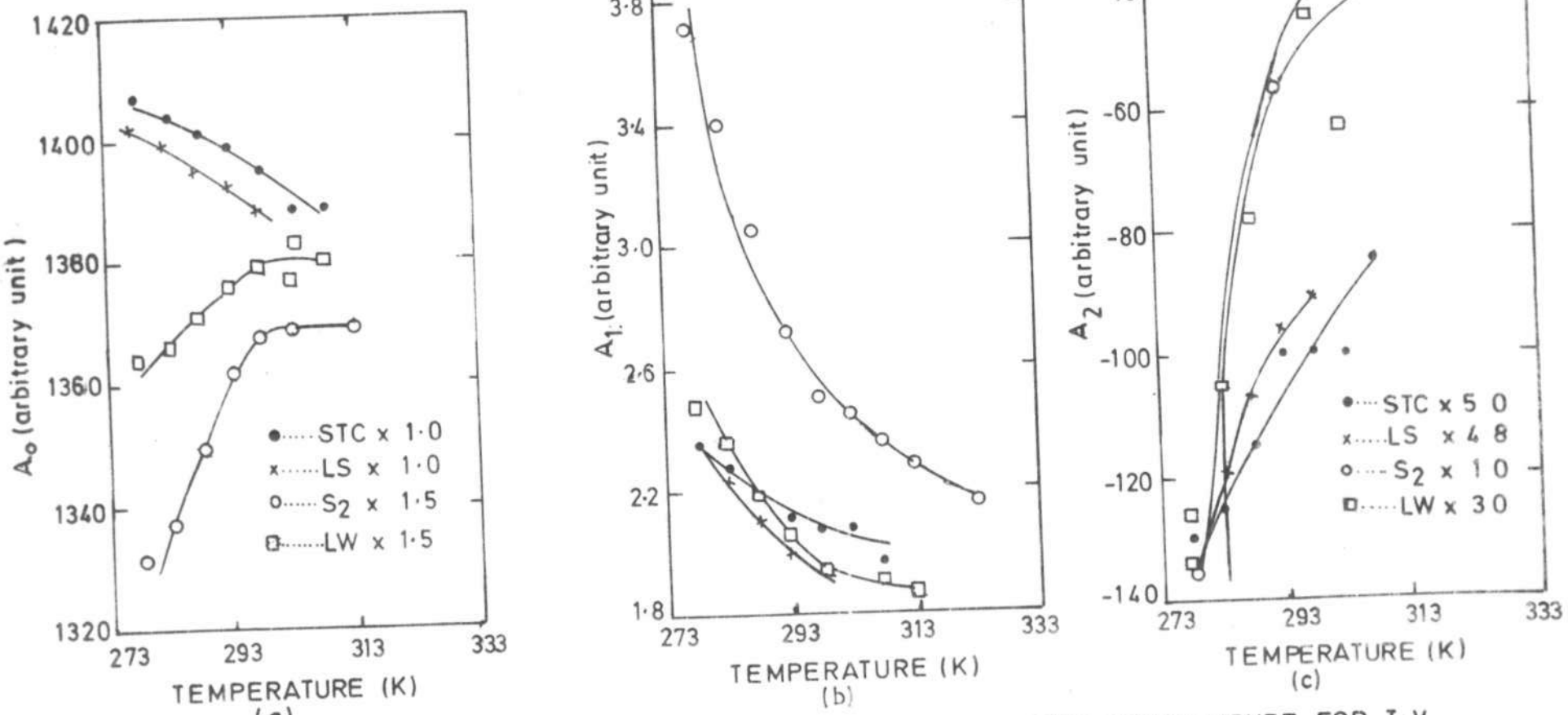

FIG 4·5: VARIATION OF POLYNOMIAL COEFFICIENTS (a) A_o, (b) A_1, (c) A_2 WITH TEMPERATURE FOR I-V CHARACTERISTICS FOR 2 TERNARY (LS, STC) AND 2 QUARTERNARY (S_2, LW) LASERS.

4.1 and 4.2. The coefficients A_o, A_2 and A_4 increase with temperature for ternary lasers but decrease with temperature for quarternary lasers. The coefficient A_3 however shows opposite variation with temperature for the lasers. Here, the coefficient decreases with temperature for ternary lasers but increase with temperature for quarternary lasers. The behaviour of these coefficients may be attributed to material composition and geometrical design of the lasers.

The coefficient A_1 shows the most significant behaviour out of these coefficients. It increases exponentially with temperature for all the lasers. Also, its variation with temperature for ternary lasers is very low compared to quarternary lasers again indicating the higher temperature sensitivity of quarternary lasers. This coefficient may be related to threshold current which also varies exponentially with temperature. It may also be related to other laser parameters such as active layer thickness, substrate doping level, facet reflectivity, heterojunction spacing etc. which exhibit well defined variation with threshold current.

4.3.2 Variation of Polynomial Coefficients with Temperature for L-V Characteristics

The graphs in figure 4.3 and 4.4 show that coefficients A_1 and A_3 increase with temperature for quarternary lasers but decrease with temperature for ternary lasers. These coefficients may therefore be related to the threshold voltage which exhibit similar variation with temperature for the two types of laser diodes. The coefficients A_2 and A_4 show the same behaviour if their absolute values are considered (i.e without their signs), and hence may also

be related to the threshold voltage.

4.3.3 Variation of Polynomial Coefficients with Temperature for I-V Characteristics

The variation of the coefficients of the fitting polynomial for this characteristics is presented in figure 4.5. The coefficient A_o increases with temperature and later reach saturation for quarternary lasers but decreases with temperature for ternary lasers. The coefficient A_1 decreases with temperature for all the lasers. This may be indirectly related to the junction series resistance which normally increases with temperature. If the absolute value of A_2 is considered, then it shows similar behaviour as A_1 and the same interpretation holds. If however the absolute value is not considered, then it shows opposite variation with temperature as A_1 and may have a direct relationship with the junction resistance.

4.4 Predictability of Temperature Sensitivity of Laser Diodes from T-I Characteristics

When the set of exponential curves in figure 3.3 were linearised by calculating the natural logarithm of current, the sets of linear graphs shown in figure 4.6 were obtained. The graphs show that the light output loci are well separated for values of current less than the threshold current and are close together for values of current greater than the threshold current.

The inserted tables in the graphs show the slope and the intercepts for various light output loci. The slopes of these graphs are approximately equal to the temperature sensitivities

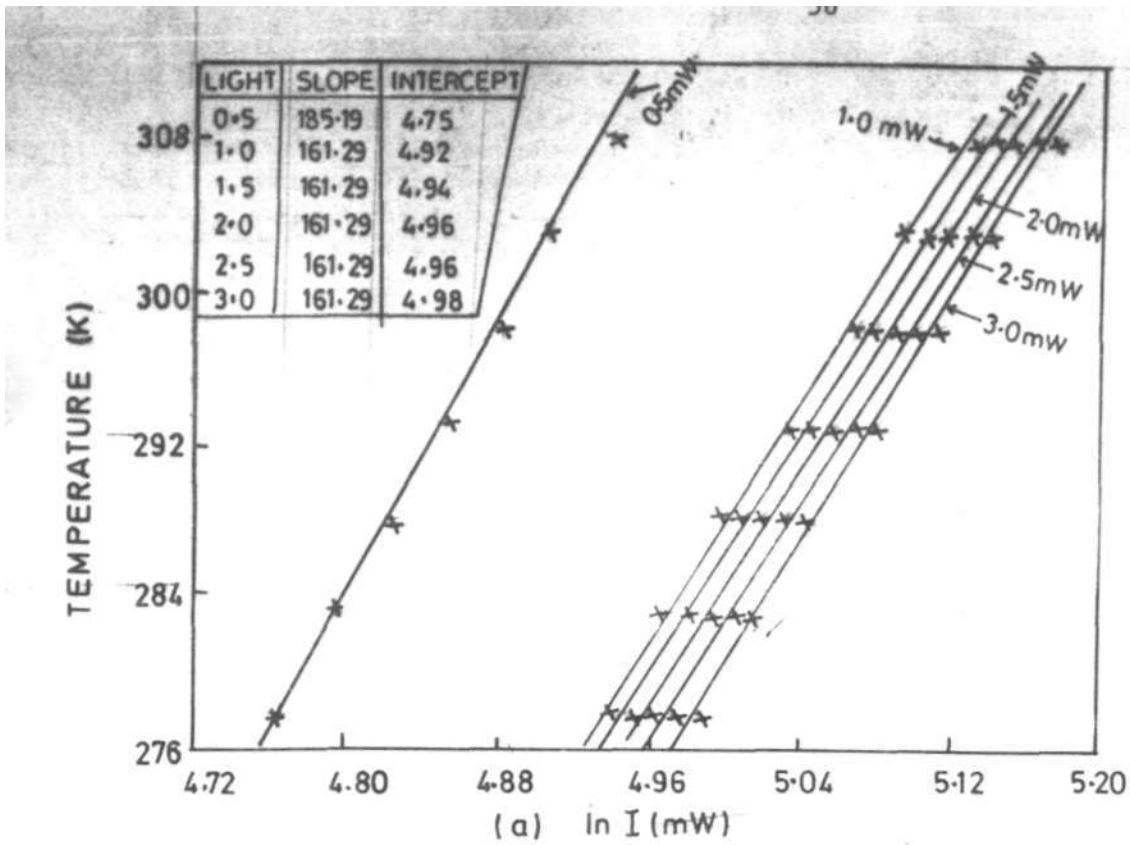

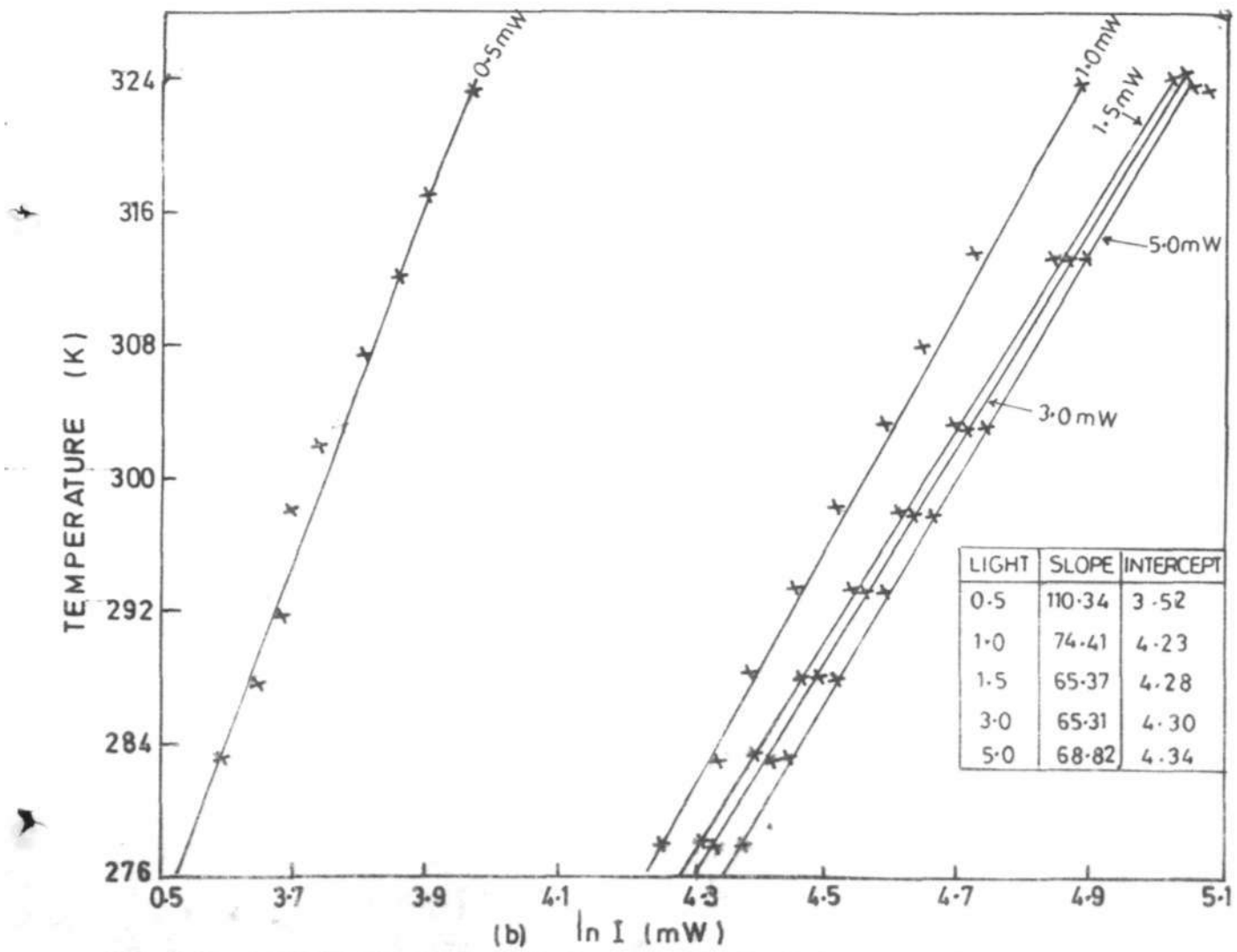

FIG 4·6: TEMPERATURE VS NATURAL LOG OF DRIVE CURRENT FOR VARIOUS VALUES OF LIGHT OUTPUT FOR (a) GaAlAs TERNARY LASER AND (b) GaInAsP QUARTERNARY

T_o of the lasers for values of current above the threshold current. For example, for a GaAlAs laser, the experimental value of T_o is 151 ± 4 while the average values of the slopes when the current is above the threshold current is 161.29 corresponding to about 3.4% difference. Similarly, for a GaInAsP laser, the experimental value of T_o is 63 ± 1 while the calculated value is 66.5 corresponding to about 3.9% difference. This method of presenting laser characteristics is expected to find application in the design of temperature modulator, current modulator and temperature sensing circuit for the laser.

4.5 Discussion

Many factors are responsible for the behaviour of laser diodes. These factors include geometrical design, bonding, active layer thickness, doping level etc. Unfortunately, comprehensive details of these laser parameters are not available for a more detailed interpretation of the results obtained.

CHAPTER 5

CONCLUSION

In Chapter 3, the electro-optical characteristics of lasers were analysed numerically by fitting polynomial equations to their respective threshold regions. It was also shown that the fitted equations correctly approximated the data, by comparing experimental data with theoretical data, in which case the two data values are almost equal, and by investigating the variation of d^2L/dI^2 with I in which the highest peak correspond to the laser threshold current.

The coefficients of the fitted equations vary with temperature, showing that the electro-optical characteristics of a laser diode cannot be easily represented by a single equation at all temperatures. The variation of these coefficients with temperature however has an interesting implication in that they can be related to temperature dependent parameters of the laser. It was shown in Chapter 4 that the threshold current, which also varies with temperature, can be calculated from a combination of these coefficients.

Another method of presenting laser diode characteristics was also derived from the L-I characteristics by linear interpolation. This characteristics called Temperature-Current Characteristics shows an exponential variation of temperature with current at constant light output and clearly indicates that the optical output of a laser is highly sensitive to current and temperature when the laser is operated above the lasing threshold.

Since the variation of threshold current with temperature is also exponential and the temperature sensitivity of the laser can be calculated from it, the temperature-current characteristics was also linearised and the slopes of the graphs approximated the temperature sensitivity when the drive current is above the threshold current. This method of representing laser characteristics is expected to find application in the design of temperature modulator and temperature sensing circuit for the laser diode.

Further analysis can be carried out in future by selective variation of the coefficients of the fitting function to change the shape of the electro-optical characteristics. From the new characteristics generated, certain laser parameters like active layer thickness, doping level etc which influence the operation and performance of laser are expected to be determinable.

REFERENCES

(1) Aghadaei, M.H., Rowlands, A.R., Buck, A.A., Kar, A., and Thomas, B. (1981). Automatic Testing of Semiconductor Laser Diodes. Proc. of the Automatic Testing Conference, Brighton.

(2) Casey, H.C and Panish, M.B. (1967). Composition Dependence of the $Ga_{1-x}Al_xAs$ Direct and Indirect Gaps. J. Appl. phys., 40, 4910.

(3) Casey, H.C. and Panish, M.B. (1978). Heterostructure Lasers Academic Press, New York.

(4) Casey, H.C. and Panish, M.B. (1978). Heterostructure Lasers, Part A and B. Academic Press, New York.

(5) Curtis, F. Gerald (1978). Applied Numerical Analysis. Academic Press, New York.

(6) Hayes, J.G. (1970). Numerical Approximations to Functions and Data. Athlone Press.

(7) Henshall G.D. (1977). The suppression of internally circulating modes in (GaAl)As/GaAs heterostructure lasers and their effects on catastrophic degradation and efficiency. Appl. phys. Lett. 31, 205.

(8) Kirkby, P.A. (1981). Semiconductor laser sources for optical communication. The Radio and Electrical Engineer. Vol. 51 No. 718 pp 362 - 376.

(9) Kobayashi, T., Furukawa Y. (1975). Temperature distributions in the GaAs - AlGaAs Double - Heterostructure Laser Below and Above Threshold. Jap. J. Appl. phys. 14, 1981.

(10) Kressel, H. and Butler, J.K. (1979). Semiconductor Laser and Heterojunction LEDS. Academic Press, New York.

(11) Kroemer, H. (1963). A proposed class of Heterojunction injection Lasers. Proc. IEEE, 51, 1782.

(12) Nash, F.R., Wagner, W.R., and Brown, R.L. (1976). Threshold Current Variations and Optical Scattering losses in (AlGa)As Double Heterostructure Lasers J. Appl. phys. 47, 3992.

(13) O'Hara, S., Huchinson, P.W., and Dobson, P.S. (1977). The Origin of Dislocation Climb During Laser Operation. Appl. phys. Lett. 30, 368.

(14) Okunade, I.O., and Oyedokun, Z.O. (1989). Predictability of Lasing Threshold in Semiconductor Laser Diodes (in press).

(15) Oyedokun, Z.O. (1985). Automatic Testing of Semiconductor Laser Diodes. (Unpublished).

(16) Oyedokun, Z.O. (1989). Current control Alogarithm in Automatic Characterisation of the Laser Diode. (in press)

(17) Oyedokun, Z.O. (1989). Data Acquisition of the Laser Diode. (in press).

(18) Oyedokun, Z.O. (1989). Integrated Automatic Test Bed for semiconductor injection lasers. (in press).

(19) Paoli, T.L. (1976). Non-linearities in the Emission Characteristics of Stripe Geometry $Al_{1-x}Ga_xAs$ Double-Heterostructure Junction Lasers. IEEE J. Quantum Electron; GE-12, 770.

(20) Ripper, J.E., Dogment, J.C., D'Asaro, L.A. and Poole, T.L. (1971). Stripe geometry double heterostructure junction lasers: Mode Structure and CW operation above room temperature. Appl. phys. Lett. 18, 155.

(21) Special Semiconductor laser conference issue (1981). IEEE J. Quantum Electron QE-17, 588.

(22) Thomas, B., Kar, A., and Henshal G.D., Jones K., (1982). Forward Bias Voltage Characteristics for (GaAl)As and (GaIn)(AsP) Lasers. IEEE Proc., Vol. 129, Pt. I, No. 6.

(23) Thompson, G.H.B., and Henshall, G.A. (1980). Non-radiative carrier Loss and Temperature Sensitivity of Threshold in 1.27 μm (GaIn)(AsP)/InP DH Lasers. Electron Lett. 16, (1), pp. 42-44.

(24) Thompson, G.H.B. (1980). Physics of Semiconductor Laser Devices. Wiley, Chichester.

(25) Wang, S. (1973). Principles of Distributed Feedback and Distributed Bragg-reflector Lasers. IEEE J. Quantum Electron. QE - 10, 413.

(26) Zory, P. (1975). Grating Coupled Double-Heterostructure AlGaAs Diode Lasers. IEE J. Quantum Electron. QE-11, 451.